S-transform Based Detection and Classification of Breast Cancer in Ultrasound Images

By

Mekdes Seyoum Abebe

In Partial Fulfillment of the Requirements for the Degree of Master of Science in Biomedical Engineering

Center of Biomedical Engineering

Addis Ababa Institute of Technology

Addis Ababa University

Advisor: Dawit Assefa Haile (PhD)

Co advisor: Mengistu Kifle (PhD)

Addis Ababa, Ethiopia

September, 2019

Declaration

I, the undersigned, declare that this MSc thesis is my original work, has not been presented for fulfillment of a degree in this or any other university, and all sources and materials used for the thesis have been acknowledged.

Name: Mekdes Seyoum Abebe

Signature: ________________

Date: ____________________

This MSc thesis has been submitted for examination with my approval as an advisor.

____

Dawit Assefa Haile (PhD)

____

Mengistu Kifle (PhD)

Certificate of Examination

Addis Ababa University

School of Graduate Studies

This is to certify that the thesis prepared by Mekdes Seyoum Abebe entitled: "*S-transform Based Detection and Classification of Breast Cancer in Ultrasound Images*" submitted in partial fulfillment of the requirements for the Degree of Master of Science in Biomedical Engineering (Bioinstrumentation and Imaging) complies with the regulations of the University and meets the accepted standards with respect to originality and quality.

Signed by the examining committee

Examiner ____________________________ Signature ________________ Date _______________

Examiner ____________________________ Signature ________________ Date _______________

Advisor _____________________________ Signature ________________ Date _______________

Co advisor ___________________________ Signature ________________ Date _______________

____

Chief of Department or Graduate Program Coordinator

Abstract

S-transform Based Detection and Classification of Breast Cancer in Ultrasound Images

Breast cancer is the second leading cause of death for women all over the world. Since the cause of breast cancer remains unknown, early detection and diagnosis is the key for control. In that regard, Breast Ultrasound Imaging (BUS) has become important modality for breast cancer detection due to its noninvasive, cost effective nature and suitability for screening and diagnosing in low resource settings.

Ultrasound imaging is one of the most frequently used diagnosis tools to detect and classify abnormalities in breast. A known drawback of the technology is that it has high amount of speckle noise which results in poor image quality. This makes it difficult to use the imaging technology for accurate detection of malignant tumors. The procedure is traditionally carried out by visual assessment of the images which is often a time taking process prone to observer variability issues. In this regard, computer aided detection techniques have been developed in various literatures showing promises with their merits and demerits. Nevertheless, image based accurate detection of breast cancer is still a topic of interest with many ongoing researches in the area.

In the current work, S-transform based breast cancer detection and classification method is developed. The proposed system consists of four stages: preprocessing, segmentation, feature extraction and classification. Image enhancement and speckle noise reduction were implemented during preprocessing. Region of interest (ROI) is then accurately determined on preprocessed images by employing canny edge detection. The ultrasound images were then classified based on different features like mean, variance, standard deviation (STD), entropy and contrast metrics. The results of the classification stage were compared against available ground truth images acquired from research image database. Accordingly, the classification procedure implemented using artificial neural network offered 90% detection accuracy.

Key words: S-transform, Breast Tumor, Ultrasound, Image Processing, Feature Extraction, Classification

Acknowledgment

First and foremost, I would like to thank the almighty God for the strength and his blessing in completing this thesis.

Next, I would like to convey my sincere gratitude to my advisor Dr. Dawit Assefa Haile for his advice, continuous support, motivation, enthusiasm, patience, constructive comments and immense knowledge throughout the process of researching and writing this thesis.

I am also grateful to my co advisor Dr. Mengistu Kifle for his academic guidance, motivation, encouragement and valuable suggestions.

I am also indebted to Dr. Masreshaw Demelash, Head of the Center of Biomedical Engineering, for his guidance and valuable advice. I also would like to say thanks to all staff members of the Center of Biomedical Engineering and all my friends for all the fun time and support in all these years.

Finally, it is my great deep appreciation to my parents for their unlimited support and continuous encouragement throughout my years of study. This accomplishment would not have been possible without them. Sincere thanks to all.

Table of Contents

List of Figures

List of Tables

List of Abbreviations

AUC	Area under the Curve
A-Mode	Amplitude Mode
ANN	Artificial Neural Network
B-Mode	Brightness Mode
BPNN	Back Propagation Neural Network
BUS	Breast Ultrasound Imaging
CAD	Computer Aided Diagnostics
CFI	Color Flow Imaging
CW	Continuous Wave
FN	False Negative
FP	False Positive
MATLAB	Matrix Laboratory
M-Mode	Motion Mode
MRI	Magnetic Resonance Imaging
PCA	Principal Component Analysis
PC	Principal Component
PDI	Power Doppler Imaging

PW	Pulsed Wave
ROC	Receiver Operating Characteristics
ROI	Region of Interest
SSS	Small Sample Size
STD	Standard Deviation
TEE	Transesophageal Echocardiography
TN	True Negative
TP	True Positive
US	Ultrasound
WHO	World Health Organization
1D	One Dimensional
2D	Two Dimensional
3D	Three Dimensional

Glossary

Benign tumor	A mass of cells (tumor) that lacks the ability to invade neighboring tissue.
Carcinoma	A cancer that starts in cells that make up the skin or tissue lining organs.
Cyst	A balloon-like sac filled with fluid, gas, or semisolid substances. A cyst is benign - non-cancerous.
Duct	A small, tube-shaped part of the body that carries fluids like breast milk.
Abscess	A collection of infected fluid within the breast tissue.
Lipomas	Is a pocket of fat that is encapsulated by a thin fibrous capsule.
Fibro adenomas	Is a lump in the breast which usually moves when you touch it.
Mastectomy	A surgical procedure of removing the entire breast.
Malignant tumor	Means that the tumor is made of cancer cells, and it can invade nearby tissues.
Mammogram	X-ray picture of the breast.
Sensitivity	It is a measure which determines the probability of the results that are true positive as that person has the tumor.
Specificity	It is a measure which determines the probability of the results that are true negative as that person does not have the tumor.
Tumor	An abnormal mass of tissue.
Ultrasound	Medical imaging that uses sound waves to make pictures of soft tissues.

Chapter 1

Introduction

1.1 Background

Cancer refers to uncontrolled multiplication of group of cells which grow at a very high rate in a particular location of the body. A group of rapidly dividing cells forms a mass of extra tissue or lamp which is referred as tumor [1][2]. Breast cancer is a form of malignant tumor which is developed from breast cells most commonly from the inner lining of milk ducts or less frequently from lobule that supply milk to the ducts. Among various types of cancers, breast cancer is the second most common and leading cause of death for women after lung cancer worldwide and more than 8% of women are affected from breast cancer during their life time [3][4][5][6]. Breast cancer starts when cells in the breast grow out of control and usually form a tumor that can be seen on x-rays as a lump [7]. The tumor is malignant if the cells can grow into the surrounding tissues or spread to distant areas of the body or benign if it is normal [8].

According to the American Cancer Society, in the United States, breast cancer has the highest incidence and death rate of all cancers in women [9][6]. A report in the United States published in 2014 showed that 29% of all new cancer cases accounts for breast cancers, the highest rate among all other cancer types [10]. In the year 2017, it was estimated that there were 252,710 new cases (30% in all cancers) and 40,610 deaths from (14% in all cancers) breast cancer [11]. WHO statistics of 2018 reported, mortality is growing especially in those regions of the world without early detection programs [12]. Early detection is the crucial step towards reducing the death rate, to have proper treatment, to improve the survival rate and prognosis since the cause remains unknown [13]. However, early detection requires an accurate and reliable diagnosis which enables identification of malignant and benign tumors [7][14][15].

Rapid and accurate assessment of tumor type is basic to enable a physician to determine the appropriate treatment options for patients. Ultrasound, Mammography and Magnetic resonance imaging (MRI) are the various diagnostic techniques used for breast cancer detection [16][15].

Over the years, the surgical treatment of breast cancer was removing whole breast in the form of mastectomy [17]. Less invasive surgical procedures were developed in recent decades in the treatment of breast cancers [17]. Previously, the most common tool for early detection and screening was mammography. Even if there are limitations to mammography, it is a medical imaging device that is used to find and diagnose breast diseases by taking x-ray image of the breast. It is done as a screening test and also if someone has problems like lump, pain, or nipple discharge. It is difficult to do examination using mammography for high risk women who have dense breast tissue and mammography shows an area of the breast that may be cancer by taking a sample of tissue and checked under a microscope to verify whether it is cancer or not [18].

However, reading mammography depends on experience, training and subjective criteria [6]. Unnecessary biopsies (65-85%) are performed due to low specificity of mammography which makes the patient suffer from emotional pressure and also increase the cost for treatment. Approximately 65% of cases referred as surgical biopsies are benign lesions (not malignant) [19]. In addition, mammography has radiation hazard and not accurate in detecting breast cancer due to its sensitivity [13]. Mammography hardly detects breast cancer in adolescent women with dense breasts and the ionizing radiation of mammogram can increase the health risk for radiologists and patients [7].

Lately, MRI became useful and an important imaging modality used for breast tumor visualization and detection [20]. The moderate specificity rate of MRI imaging increases its false positive percentages [20]. Diagnosis of specific type of cancer at its early stages would have higher sensitivity rates if MRI is used for routine examination [20].

Currently, an alternative to mammography employed for breast cancer detection is ultrasound imaging. Even though it has limitations such as low contrast and low resolution, blurry edges between various tissues and presence of speckle noise, there is an increasing interest to use ultrasound imaging for breast cancer detection [19]. Ultrasound imaging has been highly used to detect breast cancers mainly because it is radiation free, cheaper and capable of forming real time imaging [10]. Previous studies showed that the use of ultrasound can increase overall cancer detection by 17% and reduce unnecessary biopsies by 40% which can save as much as $1 billion per year in the United States only [7].

Breast ultrasound imaging is superior since ultrasound examination is more convenient, it involves no radiation and is safe compared to mammography. For detecting abnormalities in breast, ultrasound is more sensitive than mammography and it is more valuable for women younger than 35 years old. Ultrasound is useful for deeper look of breast masses and it could identify if a suspicious area is cyst or other lesion [21]. However, ultrasound is much more operator dependent than mammography. Reading ultrasound images requires well trained and experienced radiologists [6]. In addition, it suffers from a number of shortcomings such as ambient noise from the environment, acquisition noise from the equipment, anatomical influences such as body fat and breathing motion and the presence of background tissue [22]. As a result assessment of ultrasound images in the clinics is subjective (because of observer variability issues). Furthermore, the procedure is often time consuming. This calls for the development of automated tools that could be used in assessing the ultrasound images more effectively and efficiently.

Recently, several approaches have been studied to minimize the effect of operator-dependent nature inherent in ultrasound imaging and also to increase the diagnostics specificity and sensitivity. Diverse classification algorithms including decision tree, computer aided diagnostics (CAD) system and Artificial Neural Network (ANN) have been widely used for mass detection and classification of breast tissues based on ultrasound imaging. Most of the currently used algorithms are based on CAD, whose performance is affected by short comings of small sample size (SSS) problem with limited labeled instances by pathological examination [23].

In medical ultrasound imaging, the generated sound wave is transmitted into the body and the reflected echoes are converted to electrical signal by piezoelectric crystal which is then processed by ultrasound machine to create images of the internal structures of the body. This test is noninvasive technology with no radiation harm, painless, operator friendly and inexpensive [24].

Breast ultrasound is a noninvasive and real time diagnostic examination protocol that produces images which can be used to evaluate breast lesions which are found during different examinations like screening of breast tissue, lump, cyst, muscle layers, abscess, ducts, breast masses, lobes, lipomas, fibro adenomas and even blood flow. The examination is mostly employed together with mammography [22].

The current study involves developing a new methodology for use in detection and classification of breast tumors based on the Stockwell (S) transform of ultrasound images. The intent is to develop an automated scheme that could improve the diagnostic accuracy of breast cancer by differentiating malignant and benign tumor based on effective analysis of ultrasound images. The general requirements for ultrasound image denoising are effective reduction of speckle noise, contrast enhancement and extraction of useful information [23]. In that regard, effective denoising of the ultrasound images is mainly considered in this thesis while speckle noise was given emphasis.

1.2 Statement of the Problem

Detection of solid tumors, whether it is benign or malignant, is often difficult in breast ultrasound images. Identifying the exact size and coverage of tumors is also challenging in breast ultrasound due to the speckle noises in the images. It takes minutes to get ultrasound images of a subject and more time to view the images generated on a screen and carry out visual assessment. Ultrasound images are typically low contrast, low resolution, show blurry edges between various organs and are affected by speckle noise. The presence of speckle noise results in low contrast of the images which suppresses important details. Generally speaking, ultrasound is much more operator dependent than mammography. Reading ultrasound images requires well trained and experienced radiologists. Visual assessment of the ultrasound images is subjective, often time consuming and hardly repetitive which might give rise to inaccurate diagnosis. Furthermore, physicians often carry out biopsy or surgery taking a sample breast tissue to verify existence of breast cancer examining the stained sample under a microscope. There is no mechanism that detects tumors and classifies the tumors as malignant or benign in ultrasound. This could be avoided if there exists a tool that could be used for accurate detection of abnormalities in the breast automatically by clever analysis of the ultrasound images non-invasively. This calls for the development of methodology which could be used for effective analysis of the ultrasound images that could robustly detect and classify breast tumors. In this regard, the use of integral transforms has been found quit important in various literatures. Particularly, the theory of wavelets is found to be very useful in different applications. One such integral transform is the Stockwell (S) transform that showed great promises in analyzing 2D imaging signals in various disciplines. It is the intent of this thesis to investigate the applications of the S transform in analyzing breast ultrasound images and its uses in extracting features that could be used for robust classification of breast tumors.

1.3 Objectives of the Study

1.3.1 General Objective

The main objective of this thesis is to develop a methodology capable of detecting breast tumors and classifying the tumors as malignant and benign based on effective analysis of ultrasound images.

1.3.2 Specific Objectives

The specific objectives are:

- To investigate the application of the Stockwell (S) transform in extraction of useful information from ultrasound images;
- To develop an S transform based technique for use in classification of malignant and benign breast tumors;
- To evaluate the performance of the developed image analysis technique based on useful quantitative measures;
- To indicate possible clinical implications.

1.4 Significance of the Thesis

The use of mammograms in breast tissue assessment has major disadvantages. Primarily its usage of x-ray radiation might expose patients to x-ray radiation hazards. Also, accurate detection and localization of breast tumors based on mammography is often difficult. Ultrasound imaging is a useful alternative used not only to avoid use of dangerous x-rays but also to detect breast tumors. However, this requires accurate reading of ultrasound images which requires a highly specialized expertise. The task is time consuming, prone to observer variability issues and hardly repetitive. Biopsy is commonly performed on patients to verify the outcomes of the visual assessment of breast ultrasound images. The finding of this study accurately trace the location and size of breast tumors as well as classify tumors into benign and malignant thereby easing subsequent treatment of breast diseases. The use of automated techniques similar to the one proposed in this thesis is meant to circumvent such drawbacks of the visual assessment of ultrasound images. The tool is particularly more important in early detection of breast abnormalities which could lessen the risk of patients getting breast cancers.

1.5 Scope and Limitations of the Study

The methodology developed in this thesis for use in detection and classification of breast cancer has been tested on ultrasound images acquired from research image databases. The thesis studies only female breast. Stages of breast cancer is beyond the scope of this thesis. The actual clinical validation of the work is also beyond the scope of the current study. Also, the methodology developed has been implemented entirely on a Matlab platform.

1.6 Organization of the Thesis

The rest of the thesis has been organized into five chapters. Chapter 2 includes the basic concepts and the science behind ultrasound. In Chapter 3, breast tumors and breast imaging is discussed. In Chapter 4, the proposed breast ultrasound image processing algorithm is explained including the pre-processing, segmentation, feature extraction and classification steps. Results and discussions are included in Chapter 5 while Chapter 6 concludes the thesis giving some useful recommendations and possible future directions.

Chapter 2

Ultrasound Imaging

2.1 Introduction

Medical ultrasound imaging is one of the most commonly used imaging modalities for diagnostic purposes in medicine. Karl Theo Dussik from Austria was the first to use ultrasound for imaging of the brain [25]. The demand for basic and specialized ultrasound services has grown faster and got wide acceptance. Compared to other high-tech imaging protocols, the ultrasound technology is less demanding in terms of cost and consumables. However, reliable diagnostic ultrasound services require well trained and highly skilled professionals [25].

The history of ultrasound can be traced back to the time of physiologist Lazzaro Spallanzani in 1790 who experimented with bats (see Figure 1) and found that they navigate in the darkness using their hearing rather than sight [26].

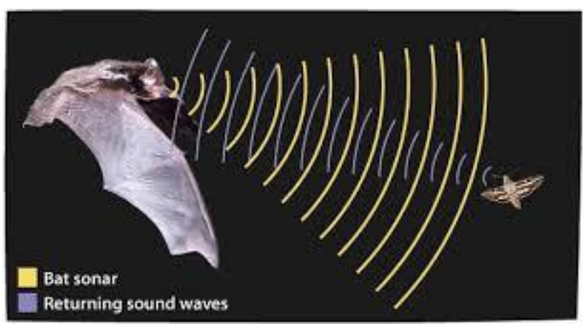

Figure 1: Bat sonar and returning sound waves [26].

Following the discovery by Lazzaro Spallanzani, many contributions were made by many scientists in the field. Inspired by the sinking of the Titanic, Paul Langevin invented a device that detects objects at the bottom of the sea called hydrophone which was able to send and receive low frequency sound waves to detect icebergs. Then after, in 1930 Karl Dussik, the Austrian psychiatrist, used ultrasound for the first time to diagnose brain tumors. In the 1950's and 60's Douglas Howry and Joseph Holmes invented a transducer that was put in direct contact with patients. In 1958, Ian MacDonald incorporated ultrasound with the obstetrics and gynecology field of medicine. John Wild and John Reid modified and produced hand held B-mode instrument which is used to detect breast tumors and also, they invented A-mode scanner for detection of ovarian cancer. In 1970s developments were led to imaging blood flow in various layers of the heart with the invention of continuous wave doppler, spectral wave doppler, and color doppler ultrasound instruments. Starting from the 1980s, ultrasound technology has become more sophisticated with improved image quality, 3D and 4D imaging capabilities. The history of ultrasound has continuously evolved and becoming more convenient into the technology we have reached today [27].

Ultrasound is a sound wave with frequency in MHz which is described by a number of wave parameters such as propagation direction, pressure density and particle displacement. If particle displacement is parallel to propagation direction, then the wave is called longitudinal wave or compression. If the particle displacement is perpendicular to the propagation direction, the wave is called transverse or shear [27].

The interaction of ultrasound waves with tissues is subject to the laws of geometric optics and it includes reflection, scattering, refraction, diffraction, absorption and interference in which all other interactions except interference reduce the intensity of ultrasound beam while interference could either increase or reduce the intensity of the beam based on whether it is constructive or destructive [27].

Ultrasound technique is based mainly on sending ultrasound waves and measuring the echoes reflected back from the medium. In the echo impulse ultrasound technique, ultrasound wave interacts with tissue and some of transmitted energy returns to the transducer for detection. Further, the reflected waves are taken up by the transducer probe, relayed to the machine and the system calculates the distance from the transducer probe to the tissue or organ boundaries using speed of sound in tissue and echo return time [28]. The machine displays the distances and intensities of echoes on the screen by forming two-dimensional image. Superficial structures such as tendons, breasts, muscles, testes and neonatal brain are imaged at higher frequencies (7-18MHz), which provides better lateral and axial resolution. Deeper structures such as kidney and liver are imaged at a lower frequency (1-6MHz) with lower lateral and axial resolution but with greater penetration [25].

The presence of speckle noise, which is signal dependent, degrades the usefulness of ultrasound imaging. The noise type is an inherent property of medical ultrasound imaging and because of the noise, the resolution and image contrast reduces which affects the diagnostic value of this imaging modality. So, speckle noise reduction is a primary preprocessing step for image processing of ultrasound images [27].

2.2 Physics of Ultrasound Imaging

Ultrasound imaging is a technique of generating images of the body using high frequency sound waves which is greater than upper limit of human hearing (>20 KHz). The frequency range used in diagnostic is often from 1MHz to 20MHz [29]. Ultrasound in medical imaging is generated in such a way that when an electric field is applied to an array of piezoelectric crystal located in a transducer, it forms electrical excitation which leads to mechanical distortion. The mechanical distortion of crystals forms excessive vibration which is prevented by backing layers and generate sound waves with short pulse length. In essence, piezoelectric crystals are used to convert electrical signal to generate pulse wave and vice versa [30].

Once produced, ultrasonic energy is focused with acoustic lens and then directed into the tissue. Along its path, the beam interacts with tissue through different processes and gets reflected at interfaces where there is a density difference between two adjoining organs (tissues). The reflected echoes are then processed to form an image as demonstrated in Figure 2 [31].

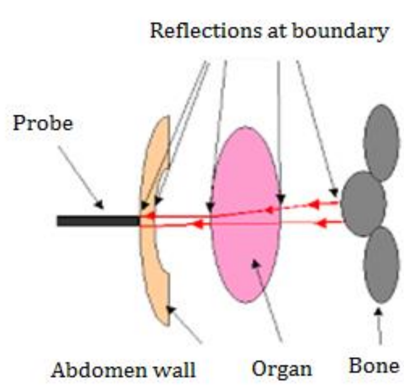

Figure 2: Principles of ultrasound [31].

2.2.1 Sound Spectrum

Sound is a mechanical form of energy which is produced by vibrating source. Frequency of vibration is the number of vibrations per time which is used to determine the quality of produced sound and is expressed in Hertz [29].

The sound spectrum can be divided into 3 parts namely audible sound, infrasound and ultrasound. Audible sounds are sounds which can be heard by human ear with frequency range from 20Hz to 20KHz. Infrasound's are sounds which can't be heard by human ear and have lower frequencies than human hearing frequency range. Ultrasounds are sounds which have higher frequencies than the upper limit of human hearing (above 20KHz) [25]. Figure 3 presents the different regions of the sound spectrum.

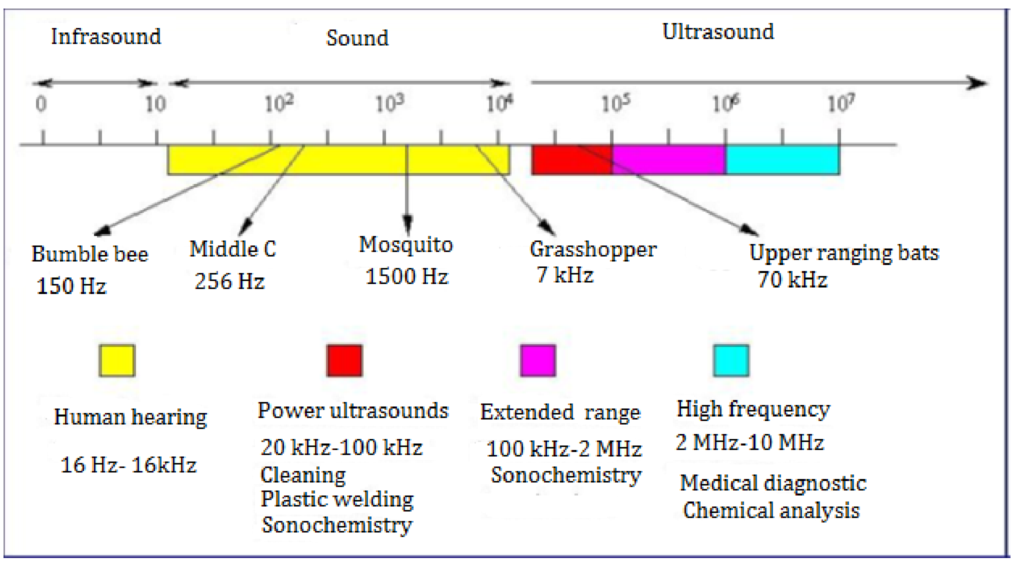

Figure 3: Sound Spectrum [29].

2.2.2 Propagation of Sound Waves

Sound is a vibration transmitted through solid, liquid or gas as a mechanical pressure wave which carries kinetic energy. A medium must present for propagation of ultrasound waves. Ultrasound propagates in a fluid or gas as longitudinal waves, in which the particles of the medium vibrate to and from along the direction of propagation, compressing and rarefying the material. In solids, such as bone, ultrasound can be transmitted as both longitudinal and transverse wave [32].

An ultrasound wave could be either longitudinal, transverse or a combination of both. Ultrasound wave propagated at the same direction with direction of oscillation is longitudinal wave. When ultrasound wave is propagating perpendicular to the direction of oscillation of source of ultrasound, it is a transverse wave. Many of biomedical applications of ultrasound are in the longitudinal category. Although ultrasound is usually propagated as longitudinal wave, in bones it may be propagated as transverse wave [33]. Figure 4 depicts longitudinal and transverse sound waves.

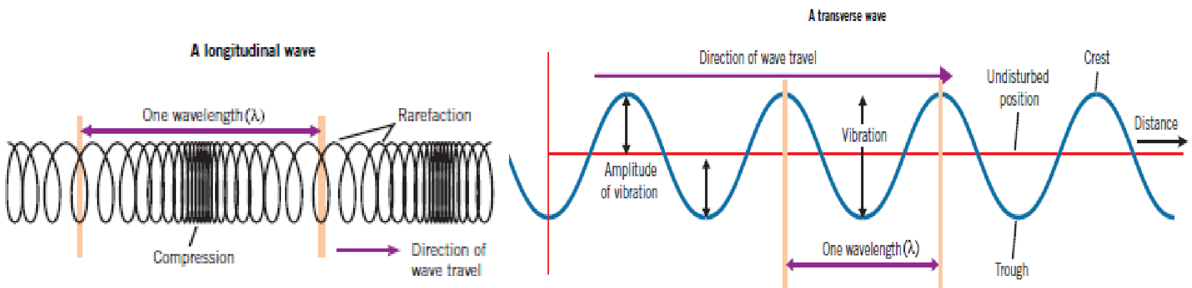

Figure 4: Propagation of sound wave: Longitudinal wave (Left), transverse wave (Right) [33].

2.2.3 Wavelength, Frequency and Period of Sound Waves

Frequency of an ultrasound wave is the number of waves passing through a given point in one second. Diagnostic ultrasound uses frequency range from 1MHz up to 20MHz but for therapeutic purposes frequency range from 200 KHz to 1MHz is used. Diagnostic ultrasound imaging depends on analysis of reflected sound waves. The resolution attainable is higher with shorter wavelengths, with the wavelength being inversely proportional to the frequency. The use of high frequencies is limited by their greater attenuation or loss of signal strength in tissue and thus shorter depth of penetration. For this reason, different frequency range is used for examination of different parts of the body [28].

Wavelength of ultrasound wave is the distance sound travels during a period of one vibration. Frequency of ultrasound for medical imaging is measured in Megahertz (MHz). Figure 5 depicts the wavelength, frequency and period of a typical sound wave with a given amplitude [33].

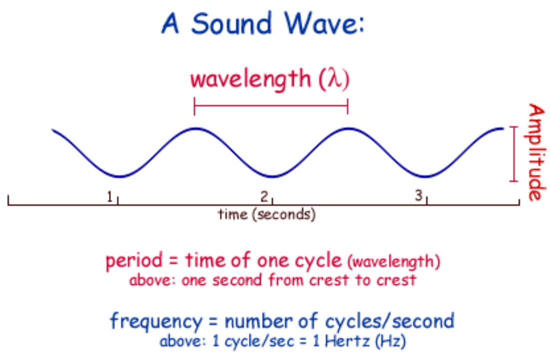

Figure 5: Wavelength, frequency and period of sound wave [33].

2.2.4 Velocity of Ultrasound

The rate at which ultrasound wave is propagated through a medium is called wave velocity. Depending on the elastic properties of the material, velocity varies from one medium to another. The velocity of ultrasound depends on the density and compressibility of the medium. The mass content of medium particles is affected by density. Denser materials are composed of more massive particles. The propagation of ultrasound wave is associated with periodic movement of medium particles. The more massive a particle is, the greater is its inertia. The larger force required to overcome particle inertia in denser materials leads to wave velocity should be lower in materials of high density. Because of the role of compressibility, this conclusion may contradict common experience [34].

Compressibility refers to the ease with which a medium can be mechanically deformed and reformed. There is a relationship between density and compressibility. Since particles are further apart, materials of low density such as gas are easier to compress. They have high compressibility. In contrast, high density materials have low compressibility. In a material of low compressibility such as bone, closeness of particles to one another implies that only slight movement of particles is required for transfer of energy to their neighbors. This predicts a higher wave velocity in a materials of low compressibility. Wave velocity represents the combined effects of medium density and compressibility. Table 1 relates wave velocity in different materials with different densities. Among these materials, velocity is lowest in air and highest in bone. While the higher density of bone predicts reduced velocity of ultrasound, its lower compressibility increases the velocity [32].

Table 1: Density and speed of sound of materials and tissue [34].

Material	Density((kg/m^3)	Velocity(m/s)
Air	1.2	330
Lung	300	600
Fat	924	1450
Water	1000	1480
Soft tissue	1050	1540
Kidney	1041	1565
Blood	1058	1570
Liver	1061	1555
Muscle	1068	1580
Skull bone	1912	4080

2.2.5 Acoustic Impedance

Ultrasound waves travel at different speed in different tissues because different tissues have different resistance to sound waves. Acoustic impedance is the measure of resistance of particles of the medium to mechanical vibrations. The resistance that a material offers is directly proportional to the density of the medium and velocity of ultrasound in the medium [32].

Acoustic impedance is used for determination of acoustic transmission and reflection at the boundary as well as the absorption of sound in a medium. The acoustic impedance (Z) depends on the density (d) of the medium and the sound velocity (c) in the medium, as shown in equation 2.1. It is measured in rayls [27]. Table 2 lists acoustic impedances of different materials.

$$Z = d.c \quad \text{(Eq:2.1)}$$

Table 2: Acoustic impedance of materials [32].

Material	Speed (m/s)	Acoustic impedance (rayls)
Air	330	0.0004×10^6
Aqueous humour	1,500	1.50×10^6
Blood	1,570	1.61×10^6
Bone	3,500	7.80×10^6
Brain	1,540	1.58×10^6
CSF	1,510	–
Fat	1,450	1.38×10^6
Lens of eye	1,620	1.84×10^6
Muscle	1,580	1.70×10^6
Skin	1,600	–
Soft tissue average	1,540	1.63×10^6
Vitreous humour	1,520	1.52×10^6

From the above table, one can conclude the followings:

- Since the acoustic impedance value between soft tissues is much similar to one other, small echoes will be generated at the boundary between soft tissues.
- The acoustic impedance value of gaseous materials is much lower than soft tissues and hence large echoes will be generated at the junction between soft tissue and gaseous materials.

2.2.6 Acoustic Boundaries

In ultrasound interaction, the values of acoustic impedance changes with the position of tissues. This boundary is named as acoustic boundary or interface. The acoustic boundary affects a beam of incident ultrasound when there is magnitude difference between acoustic impedance values of two structures on either side of the boundary [25].

2.2.7 Interaction of Ultrasound with Medium

A beam of ultrasound must be directed into the tissue in order to use ultrasound for diagnostic or therapeutic purposes. Along its path, the ultrasonic energy interacts with tissue.

Reflection of Ultrasound Waves

In ultrasound wave, reflection occurs when there is acoustic impedance difference between two adjacent tissues (see Figure 6). Depending on the size of the boundary relative to that of ultrasound beam, there are two types of reflectors. When the boundary is smooth and larger than beam dimension, it is called specular reflection. If the boundary is smaller than the beam, it is called non-specular reflection. In specular reflection, angle of incidence is equal to angle of reflection while incident beam is directed in many directions in non-specular reflection [25][32].

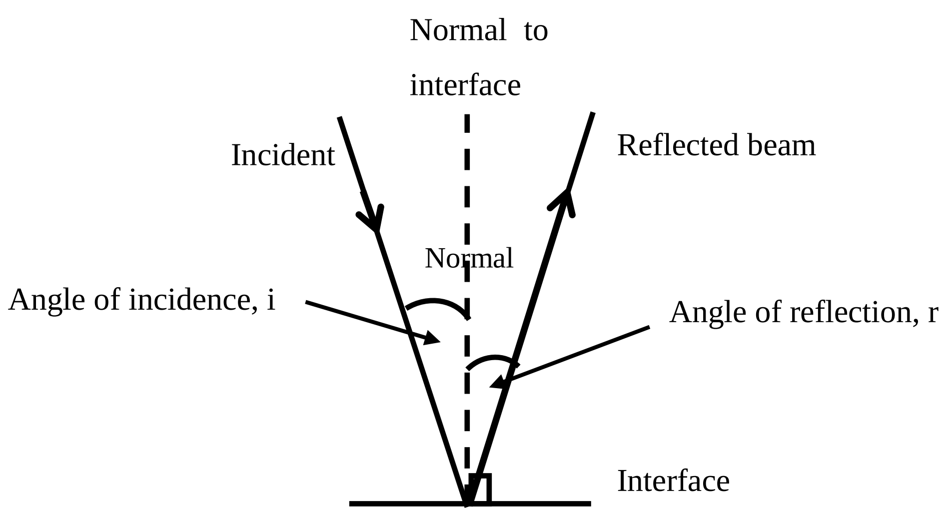

Figure 6: Reflection of Sound wave [32].

Refraction of Ultrasound Waves

When an ultrasound wave travels and crosses a tissue boundary between two media at different velocities by bending of waves, it is called refraction (see Figure 7). The path of the wave is deflected as it crosses the boundary of the media. Diffraction is basically the bending of waves around obstacles. The frequency of the beam remains unchanged while there is a wavelength change when it crosses from one media to the other [27][30]. The velocity is the product of the frequency and the wavelength.

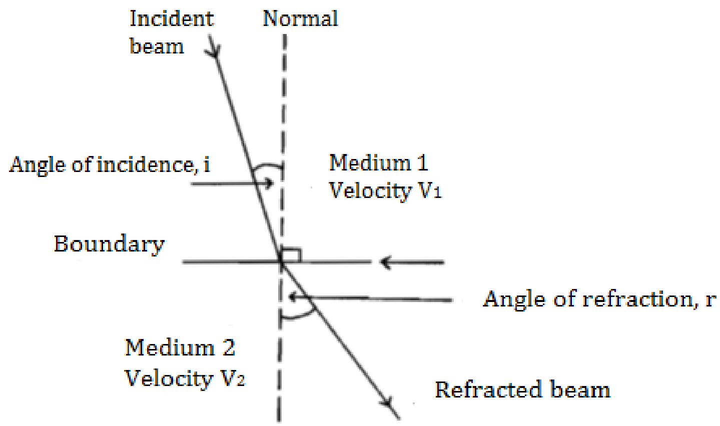

Figure 7: Refraction of ultrasound wave [30].

The relationship between angle of incidence and angle of refraction is described by Snell's law.

$$\frac{\sin I}{\sin R} = \frac{V_1}{V_2} \qquad \text{(Eq. 2.2)}$$

Where I = angle of incidence, R = angle of refraction, $V1$ = velocity of ultrasound in medium1, and $V2$ = velocity of ultrasound in medium 2.

Refraction is not useful for the process of image formation unlike reflection.

Absorption of Ultrasound Waves

Absorption is the process by which particles that transmit sound waves vibrate and cause friction which lead to loss of sound energy and production of heat when sound travels through a soft tissue. Energy is absorbed by the medium from the ultrasound beam [27][25].

The absorption by the medium is affected by the following factors:

- Viscosity of the medium,
- Relaxation time of the medium, and
- Beam frequency.

When particles move past one another, the frictional force between the medium is called viscosity. More heat is generated by the particles as the frictional force becomes greater. Absorption of ultrasound is directly proportional to viscosity. As viscosity increases, the absorption of ultrasound increases. The time taken by the medium particles to revert to their original mean position is called relaxation time of the medium. Vibrating particles are able to revert to their original position before the next disturbing pulse when the relaxation time is short. Relaxation time of the medium is directly proportional to the absorption of the medium. As the relaxation time increases, the absorption of ultrasound wave becomes higher.

More frictional heat is generated in higher frequency which leads to medium particles to move fast each other. Absorption of ultrasound is directly proportional to the beam frequency. Increasing in the beam frequency leads to higher frequency [25][31].

Scattering of Ultrasound Waves

Redirection of ultrasound wave is caused when reflecting interface is rough surface and dimension of ultrasound beam is greater than dimension of reflecting surface (see Figure 8).

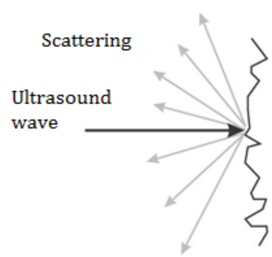

Figure 8: Scattering of ultrasound wave [31].

Attenuation of Ultrasound Waves

Attenuation is the loss in energy and intensity as ultrasound pulses are traveling through tissues. Attenuation occurs due to reflection, scattering and absorption. It is directly proportional to the frequency and distance the wave travels. The higher the frequency, the more attenuation, and the longer the penetration depth, the more the attenuation [25].

2.3 Generation and Detection of Ultrasound Pulses

2.3.1 The Piezoelectric Phenomenon

The most common method of generating ultrasound relies on a phenomenon called piezoelectric effect. This phenomenon involves reversible conversion of two types of energy namely electrical and mechanical. Piezo refers to pressure. When mechanical stress (mechanical pressure) is applied, crystals of piezoelectric materials stretch or compress applying electrical voltage on the surface and we have a crystal that can conduct an electric current. In this time, mechanical energy is converted into electrical energy and the process is called piezoelectric effect. The crystal will respond by contracting or relaxing when potential energy (electric current) is applied on it and converts electrical energy to mechanical energy which is called reverse piezoelectric effect [25].

2.3.2 Generation and Detection of Ultrasound Pulses

The generation and detection of ultrasound pulses rely on piezoelectric effect. Detection of ultrasound is based on piezoelectric effect and generation of ultrasound pulses rely on reverse piezoelectric effect. Because of its phenomena of reversibility, the same crystals can be used for production and detection of ultrasound pulses [31].

2.4 Ultrasonic Transducers

Transducer is a device which converts one form of energy to another. There are different components of transducer (also called ultrasonic probe) assemblies.

Crystal: is the key component of a transducer that is found near the front surface of the transducer and it has thin disk piezoelectric material. The crystal material has natural piezoelectric property and each crystal is called an element. The more the number of elements, the higher the ultrasound image quality. There are transducers with 64, 80, 96, 128, 192, 256 or more elements. And also, there are piezoelectric crystals artificially induced from a combination of thermal and electrical treatment. If the crystal is heated at high temperature, the piezoelectric property of artificial crystal will be destroyed. The front and back surface of crystals are coated with electrical conducting material for connections with electrodes. Electrical stimulator is placed on the front side of the transducer which has direct contact with the patient [35].

The thickness of crystals controls frequency of vibrations. Ultrasound waves are transmitted in both directions of vibrating crystals.

$$Frequency = \frac{Velocity\ of\ ultrasound}{Wavelength} \qquad \text{(Eq. 2.3)}$$

$$Wavelength = 2 \times thickness \qquad \text{(Eq. 2.4)}$$

This results in $f = \frac{V}{2T}$

where f is the frequency, V is the velocity and T is the thickness .So, the thicker the crystal, the lower the frequency and the thinner the crystal, the higher the frequency. Figure 9 presents typical piezoelectric crystal element types: curvilinear, linear and sector.

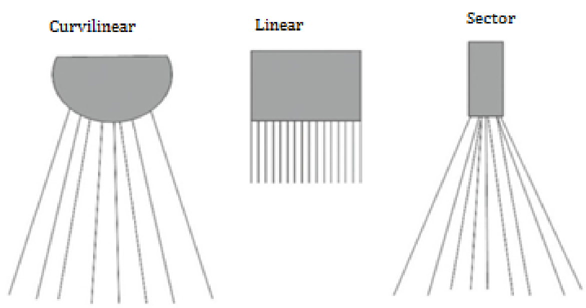

Figure 9: Piezoelectric Crystal elements [35].

Acoustic Lens: acoustic lens is used to focus the sound beam as depicted in Figure 10.

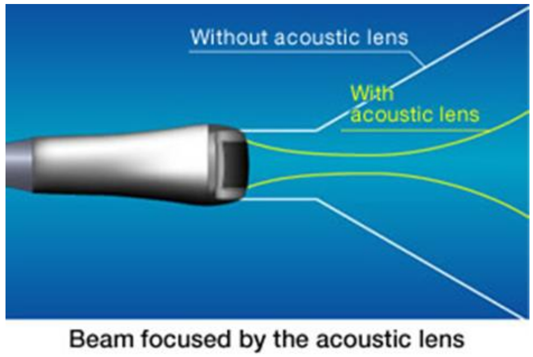

Figure 10: Acoustic lens [35].

Matching Layer: matching layer is placed in front of the piezoelectric crystal and it is used as a buffer area between piezoelectric crystal and patient body to prevent reflection of transmitted sound wave to transducer housing (see Figure 11).

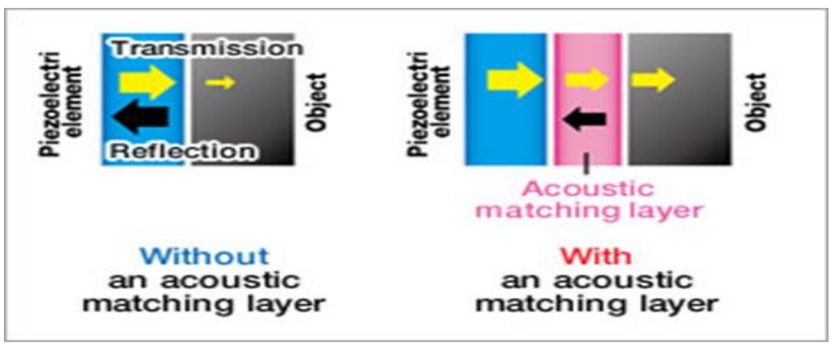

Figure 11: Matching Layer [35].

Backing Layer: backing layer is made from material which absorbs ultrasound highly and placed behind the piezoelectric crystal and it is used to prevent excessive vibration in the production of sound wave and also used to have short pulse length.

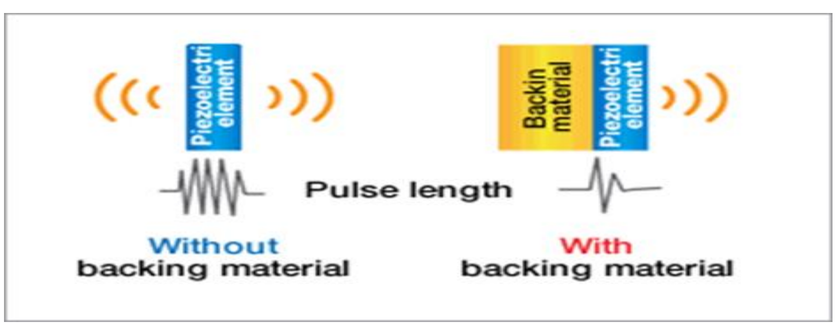

Figure 12: Backing Layer [35].

Electrodes: Electrodes are used to send and receive electrical pulse signal and send them back to a computer system.

Transducer Housing: Robust housing is used to cover internal components of the transducer.

2.4.1 Types of Transducers

Transducers are made of crystal elements which are insulated from each other. An array is geometrical configuration of crystals used to provide desired field of view. A method of providing instantaneous beam which results in crystal elements to be pulsed one at a time is called sequential pulsing. A method of providing instantaneous beam which results by excitation of group of crystals is called segmental pulsing. During ultrasound imaging, a scan line is generated by the crystal elements by their own. For example, a transducer with 80 crystal elements will produce 80 scan lines which then generates images [25].

Linear Transducer

In this case, the crystal elements are aligned in a linear fashion, the shape of the beam is rectangular, the near field resolution is good and segment of crystals are stimulated in a group to produce an ultrasound beam (see Figure 13). The produced ultrasound beam moves sequentially along the transducer one element at a time to obtain the image with uniform beam density. In linear transducers, each element produces a scan line that generates rectangular field of view image [36].

Figure 13: Linear transducer [36].

The footprint, frequency and applications of the linear transducer depend on whether the product is for 2D or 3D imaging. It is used for various scanning applications such as thyroid, appendix, vascular, breast and small parts. Its central frequency is 2.5 MHz-12 MHz [36].

Convex Transducer

In convex transducers the crystal elements are arranged in curvilinear as shown in Figure 14. The beam shape is convex and the transducer is good for in depth examinations even though the image resolution decreases with the depth increases. As the distance from the transducer varies, the ultrasound beam shape and size vary. The footprint, frequency and applications of the linear transducer depend on whether the product is for 2D or 3D imaging. Convex transducer for 2D imaging has a wide footprint and its central frequency is 2.5MHz to 7.5MHz [36].The convex transducer for 3D imaging has a wide field of view and a central frequency of 3.5MHz to 6.5MHz.It is used for various applications such as abdominal, gynecology and obstetrics examinations [36].

Figure 14: Convex transducer [36].

Phased Array Transducer

This transducer is named after the piezoelectric crystal arrangement which is called phased array, in linear or curvilinear fashion (see also Figure 15). This type of transducer uses low frequency and its central frequency is 2MHz to 7.5MHz. It has triangular beam shape and the near field resolution is poor. It is used mostly in cardiac, abdominal and brain examinations [25].

Figure 15: Phased array transducer [36].

Pencil Transducer

It is also called CW Doppler probe, utilized to measure blood flow and speed of sound in blood. This probe has a small foot print and uses low frequency (typically 2MHz -8MHz) [36].

Figure 16: Pencil transducer [36].

4D (Volumetric) Transducer

3D imaging allows fetal structures and internal anatomy to be visualized as static 3D images. However, 4D ultrasound allows to add live streaming videos of the images, showing the motion of the fetal heart wall or valves, or blood flow in various vessels. It is thus 3D ultrasound in live motion.Volumetric transducers are mostly used in obstetrics. It uses frequency range of 3.5-6.5MHz (see Figure 17) [36].

Figure 17: Volumetric Transducer [36].

Endocavitary Transducer

This probes provide you with the opportunity to perform internal examinations of the patient. Therefore, they are designed to fit specific body orifices. The Endocavitary transducer include endovaginal, endorectal and endocavity transducer. Typically, they have small footprints and the frequency varies in the range of 3.5MHz-11.5MHz.Trans-vaginal means through the vagina and Trans rectal means through anal. Trans rectal probes are used for imaging of anal defects, organs in the pelvis and mostly it is used for evaluation of prostate gland in men while trans-vaginal probes are used to assess a women's ovaries, uterus, tubes, cervix and pelvic area (see Figure 18) [36].

Figure 18: Endocavity transducers: Trans-vaginal (Left), Trans-rectal (Right) [36].

TEE probe

TEE stands for trans-esophageal echocardiography (TEE) which is often employed in cardiology to obtain a better image of the heart through the esophagus. It has small footprint and is used for internal examinations. It uses higher frequency sound waves to create an image. It uses frequency range of 3-10MHz.TEE is attached to a thin tube and inserted through the mouth, down to the throat to the esophagus. Clear images of the heart structures and valves can be obtained in the esophagus because it is so close to upper chamber of the heart [36] (see Figure 19).

Figure 19: TEE probe [36].

2.5 Ultrasound Imaging Planes

2.5.1 Transverse Plane: It is a horizontal plane which divides the body into upper and lower portions. It is also called Horizontal Plane.

2.5.2 Frontal Plane: It is a plane which divides the body into front and back regions. It is also called Coronal Plane.

2.5.3 Sagittal Plane: It is a plane which divides the body into right and left portions. It is also called Median Plane.

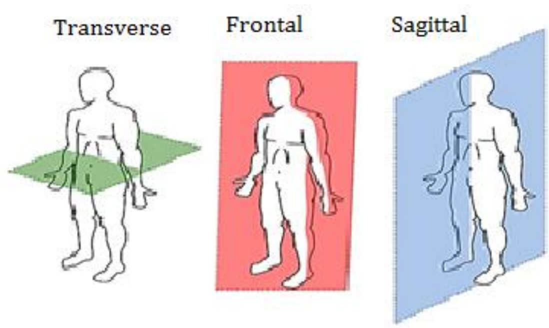

Figure 20: Imaging planes [28].

2.6 Ultrasound Imaging Modes

2.6.1 A-Mode

A- Mode stands for 1 Dimensional (1D) amplitude mode and it is a one dimensional technique in which a transducer with a single crystal is used to record returning echoes from the tissue boundaries with respect to time. Distance measurement for the tissue structure and interface can be computed using A-mode. This type of mode is mostly used in ophthalmoscopy applications and for accurate measurement of distance. There is one scan line of data generated in A-mode per pulse repetition (see Figure 21) [37].

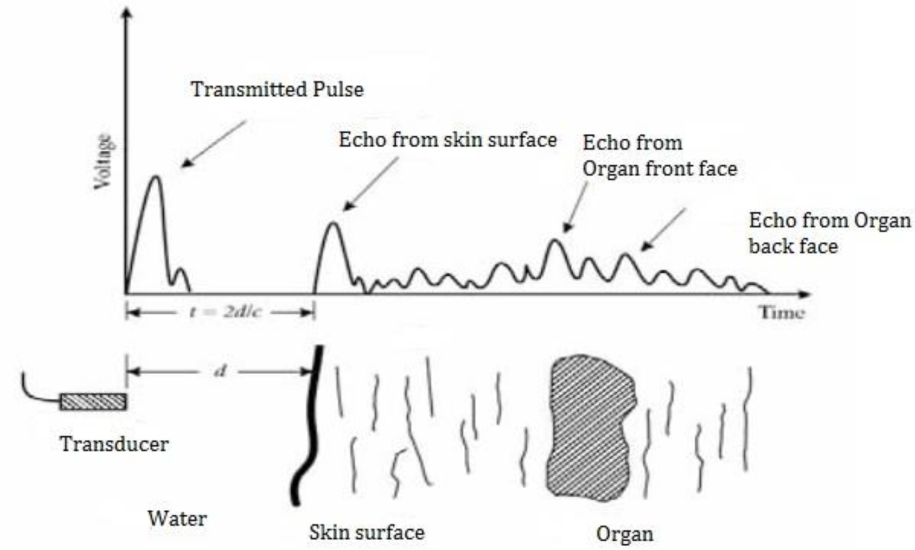

Figure 21: A-Mode [9].

2.6.2 B-Mode

B-mode is two-dimensional (2D) intensity mode. B stands for brightness and B-mode is used to provide real time gray scale two dimensional (2D) images. The brightness of B-mode images refers to the strength of reflected echoes. It converts A-mode information into brightness dots on the screen. For visualization of interface motion, sequential pulse lines are displayed adjacent to each other. The signal is having white color, intermediate signal has gray color and the absence of the signal has black color [37].

In B mode ultrasound diagnostic, the intensity of the echo is shown by modulation of the brightness of the particular spot, and the position of the echo is found from the angular position of the transducer and the transit time of the acoustic pulse and its echo. Ultrasound B- mode scans are safe and painless [37].

2.6.3 M-Mode

M stands for motion and uses B-mode to display moving structure along a single line in the image. The echoes generated by a stationary transducer are recorded continuously over time. Figure 22 shows the three ultrasound imaging modes in action.

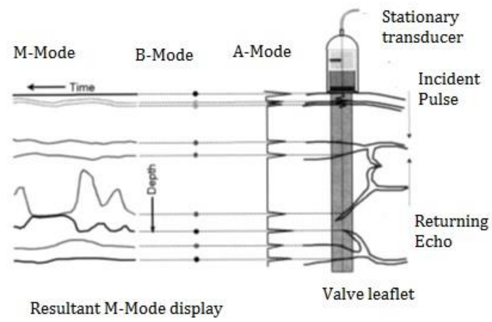

Figure 22: Ultrasound imaging modes [9].

2.6.4 Doppler Imaging

Doppler Effect: Doppler Effect is the change in received ultrasound frequency due to motion. The effect is responsible for changes in the frequency of waves emitted by moving objects as detected by stationary observer. The perceived frequency is higher if the object is moving towards the observer and lower if it is moving away. The difference in frequency (Δf_s) is called Doppler frequency shift, Doppler shift or Doppler frequency. The Doppler shift depends on the emitted frequency (f), the velocity of the object (V) and the angle (α) between the observer and the direction of the movement of the emitter as described by the formula (where c is the velocity of sound in the medium being transverse):

$$\Delta f_s = \frac{f}{c} V \cos\alpha \qquad \text{(Eq. 2.5)}$$

When the angle α is 90° (observation perpendicular to the direction of movement), no doppler shift occurs (cos 90° = 0).

Continuous wave Doppler

In Continuous wave Doppler (CW) different crystals are used to send and receive signals along a single line that is placed on the 2D image. It employs two piezoelectric crystals, both contained in a single head. One crystal transmits a continuous signal at a known frequency (3-8 MHz). The other crystal receives the returning echoes and records their frequency. In this technique, the ultrasound signal is emitted continuously. This method doesn't give any information about the location of the signal but it gives good resolution of high velocities [23].

Pulsed wave Doppler

In pulsed wave Doppler (PW) the same crystal is used to send and receive signals. In this technique, the ultrasound signal is emitted in very short pulses. The velocity and direction of flow is measured from the Doppler signal arised from a specific position in a signal [23].It provides the means of detecting the depth at which a returning signal has originated. The depth can be positioned at any point along the axis of the ultrasound beam [23].

Color Flow Imaging (CFI)

It is also called color velocity imaging or color flow imaging (CFI). The echo signals received along a series of locations in an ultrasound beam width by applied transmitted/received pulse signals called pulse packets which are used to produce an estimate of mean velocity of all reflectors along multiple beam lines in the beam width. The machine assigns color for the data and it is superimposed on B mode data from stationary structures within the beam width. Faster flow depicts brighter shades in color. The direction is conventionally denoted by assigning blue color away from the transducer and red color to flow direction towards the transducer [23].

Power Doppler Imaging (PDI)

Color flow imaging displays scattered velocities relative to the interrogating ultrasound beam direction at positions throughout the field of scan. An alternative processing method, which ignores the velocity and simply estimates the strength/amplitude of the Doppler signal detected from each location is energy mode or power mode imaging. The power mode imaging is continuous and not sensitive to relative flow direction as well as it doesn't give the absolute values of velocity but only gives the strength of the Doppler signal [23].

Thus, the advantages of Power Doppler over Color flow imaging are:

(a) More sensitive to flow states,

(b) Angle effects are ignored unless the angle is close to 90° so as to reduce Doppler signal level below threshold detection, and

(c) Inability to detect Doppler frequencies beyond a particular level from a given depth and on the set of operating conditions. This limitation is not applicable to Power Doppler Imaging.

Spectral Doppler

This type of display is typically used in vascular flow imaging by duplex scanning means (B mode + Pulsed wave Doppler) where in a sampled volume of blood flow, the Doppler signal is complex in nature. In other words, each of the velocities sampled in the beam will have different amplitude and phase, thus the final character of the sampled signal will have contributions from each of these velocities. Thus, analysis of the entire spectrum provides in assessing the characteristic of vascular flow [23].

Chapter 3

Breast Tumors and Breast Imaging

3.1 Anatomy of the Breast

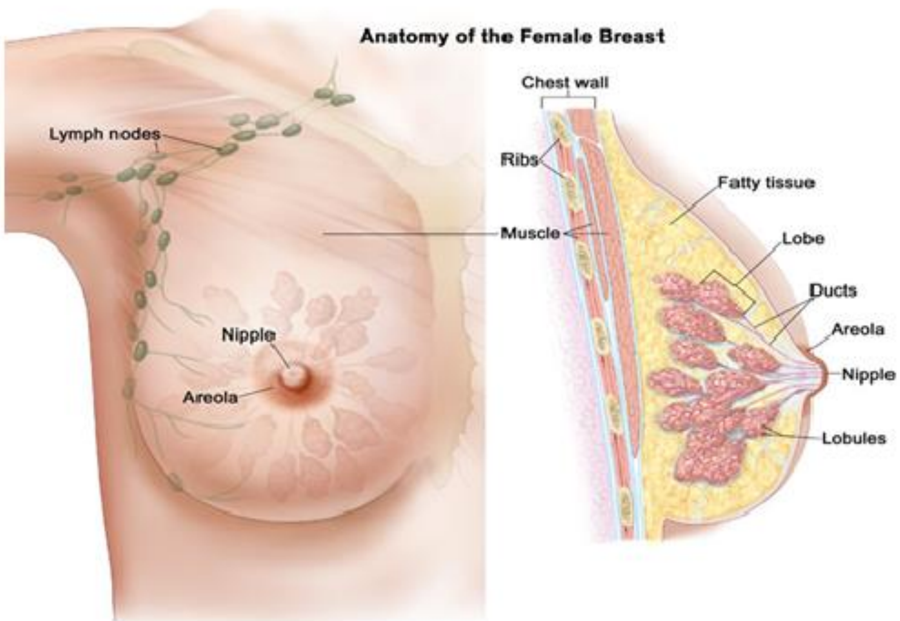

Figure 23: Anatomy of the female breast [11].

Figure 23 presents the anatomical composition of the female breast. Breast is attached to pectoral muscle of front chest wall by fibrous strands called ligament on either side of the sternum. Breasts are made up of ducts, lobules, fatty and fibrous connective tissues and contains no muscle tissue. Composition of the breast includes milk glands (lobules), ducts, nipple, areola, connective (fibrous tissue) and fat. Lobules are called glandular tissue and they are used for production of milk. Milk is transported from lobules to nipple by ducts. The brown pigmented region that surrounds the nipple is called areola [11][38]. The glands are surrounded by a layer of fatty tissue which extends throughout the breast. A soft consistency of breast is due to the fatty tissue.

3.1.1 Development of the Breast

In the 6^{th} week of fetal life, human breast tissue starts developing. Breast tissue initially grows along the lines of armpits which is then extended to groin by the 9^{th} week of the fetus, leaving two breast buds on the upper half of the chest, it goes back to chest area. From each breast bud, columns of breast grows inward and becoming separate sweet glands with ducts leading to the nipple. At birth, breast of male and female are the same and not well developed. In early puberty, breast begin to fill out and areola becomes prominent bud. In late puberty, areola becomes fat and glandular and fat tissue increase in the breast. Male's breast contains fat with glandular tissue, while female breast contains glandular tissue, acini, ducts, coopers ligament, and Montgomery's gland in addition to the male. The signal of development of glandular breast tissue is the production of estrogen and progesterone hormones. Factors that influence the women breast size are volume of breast tissue, family history, age, weight loss or gain, thickness and elasticity of breast skin, degree of hormonal influence on the breast and history of pregnancies [38].

In normal breast ultrasound image, skin appears white, fat lobules appear gray, coopers ligaments appear white, fibro glandular tissues appear white, ducts are not visible or black if dilated, chest wall ribs appear white with shadowing and fascia appears white [39].

3.2 Breast Density

Breast density is the product of fibrous and glandular tissues distributed in breast versus how much your breast is made up of fatty tissue. If there is a lot of fibrous and glandular tissues but not fatty tissue it is called dense breast. Dense breasts are linked to high risk of breast cancer but they are not abnormal. Breasts are heterogeneously dense, which may obscure small masses and they are extremely dense. What makes it harder to find cancer in breast is because it has a lot of fibrous and glandular tissues [40]. Dense breast is not abnormal, some breasts have small density due to age and others have large density. Breast density is not dependent on breast size or firmness. Women with dense breast tissue have high risk for cancer than women with low breast density. Since breast masses and tumors both looks dark in ultrasound, the denser the breast, the more the tumor is hidden. Previous studies have indicated that there is no concrete reason for this [17].

Breast density is identified by only mammography. It is classified by radiologists using 4-level density scale as shown in Figure 24: entirely fatty, scattered areas of fibro glandular density, heterogeneously dense and extremely dense.

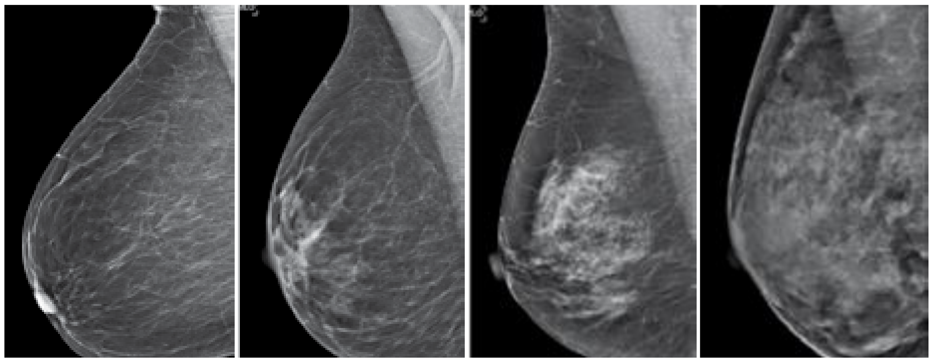

Figure 24:(a) entirely fatty (b) scattered areas of fibro glandular density (c) heterogeneously dense (d) extremely dense [40].

Entirely fatty refers to almost all the breast is composed of fatty tissue. Scattered areas of fibro glandular density refers the majority of breast tissue is nondense but there are some scattered areas of density. Heterogeneously dense refers when more than half percent is dense and the rest is fatty tissue. In extreme dense breasts, it is difficult to see tumors in the tissue. It is difficult to see tumors around the dense tissue when the breast is made of dense glandular and fibrous tissue. The risk of breast cancer increases on women who have dense breast tissues [41].

3.3 Breast Cancer

3.3.1 Overview of Breast Cancer

Breast cancer is a type of cancer which occurs when a malignant tumor forms from uncontrolled growth of cells within the breast. It arises most commonly from milk ducts of breast tissue and sometimes from lobules that supply milk to the ducts [21]. Even if men can develop breast cancer, most frequently it occurs in women [42]. Breast cancer is the second leading cause of death for women all over the world. Since the cause of the disease remains unknown, early detection and diagnosis can increase the success of treatment, save lives and reduce cost. If detected in early stages, survival rates are nearly 100%. American Cancer Society (ACS) estimates 1 in every 8 women will develop breast cancer in their life time which makes it the most common cancer types among women [43]. Another research also showed that more than 8% of women suffer with breast cancer during their life time and it is the most common female cancer in both developed and developing countries [44]. Better treatment can be provided if the cancer is early detected [45].

As they grow, the abnormal cells inside the breast often, but not always, form a tumor in the breast that can be detected on a mammogram before it can be felt as lump or thickening. Detecting of tumors in dense breasts is often carried out using ultrasound which may be missed using mammography [43]. Not all breast cancers, however, present with a lump and not all lumps in the breast are breast cancers. But all lumps or thickenings in breast need to be determined whether they are one of the many benign lumps that occur in the breast or truly cancerous [43].

Even though mammography provides detection and classification of breast cancers, many unnecessary (65-85%) biopsy operations are due to low sensitivity of mammography. The unnecessary biopsies increase the cost of treatment as well as puts the patient under emotional pressure. The ionizing radiation of mammography can increase the health risks. It also hardly detects breast cancer in adolescent women with dense breasts. Despite the fact, mammography is still used to discriminate benign and malignant masses. In mammography examination, there is a high rate of false positives which causes a lot of unnecessary biopsies. Ultrasound is one of the imaging protocols used as an alternative to mammograms. However, ultrasound is much more operator dependent than mammography which means reading ultrasound images requires well trained and experienced radiologists [21].

According to previous reports, overall cancer detection can increase by 17% using ultrasound and the number of unnecessary biopsies could be reduced by 40% which can save as much as $1billion per year in the United States. In addition, ultrasound is believed to be fit for low resource setting countries [21].

In different geographical regions of the world, breast cancer incidence, mortality and survival rates vary but incidence is increasing throughout the world. Without early detection programs, mortality is increasing. A biopsy is done when other physical exams show a breast change that may be a cancer for validation [21]. Early diagnostic and detection is key for breast cancer disease control since the cause of the disease remains unknown. Early detection of cancer also increases the success of treatment, saves life and reduces costs. Regular breast cancer screening is important because many women with breast cancer show no symptom at early stages. During screening the cancer found is mostly small [21].

3.3.2 Risk Factors of Breast Cancer

Factors that increase the risk of developing breast cancer include [41]:

Aging: A woman's chances of getting breast cancer increase as she ages.

Family history: Women with close relatives who've been diagnosed with breast cancer have a higher risk of developing the disease. If you've had one first-degree female relative (sister, mother, daughter) diagnosed with breast cancer, your risk is doubled.

Genetics: 5% to 10% of all breast cancers can be linked to women and men with gene mutations that were inherited from their mothers or fathers.

Dense breasts: Women who have a high percentage of breast tissue that appears dense on a mammogram have a higher risk of breast cancer than women of similar age who have little or no dense breast tissue.

Race: In the United States, breast cancer is diagnosed more often in white women and least often in Alaska native women.

Age, family history and genetics, late first pregnancy and obesity are well-established risk factors for breast cancer. In addition the study of Wolk et al. (1998) indicates that in many populations, polyunsaturated fats have a greater cause of breast cancer [11]. Figure 25 and 26 present patterns of distribution of breast cancer incidence and mortality across the globe [41].

Although breast cancer incidence, mortality and survival rates vary in different geometrical regions, its incidence is increasing as a world as whole. As per statistics of WHO in 2018, shown in Figure 25, increased risk of incidence rates arises in countries of higher socioeconomic conditions and as Figure 26, increased risk of mortality rates is growing in those regions of the world without early detection program [41].

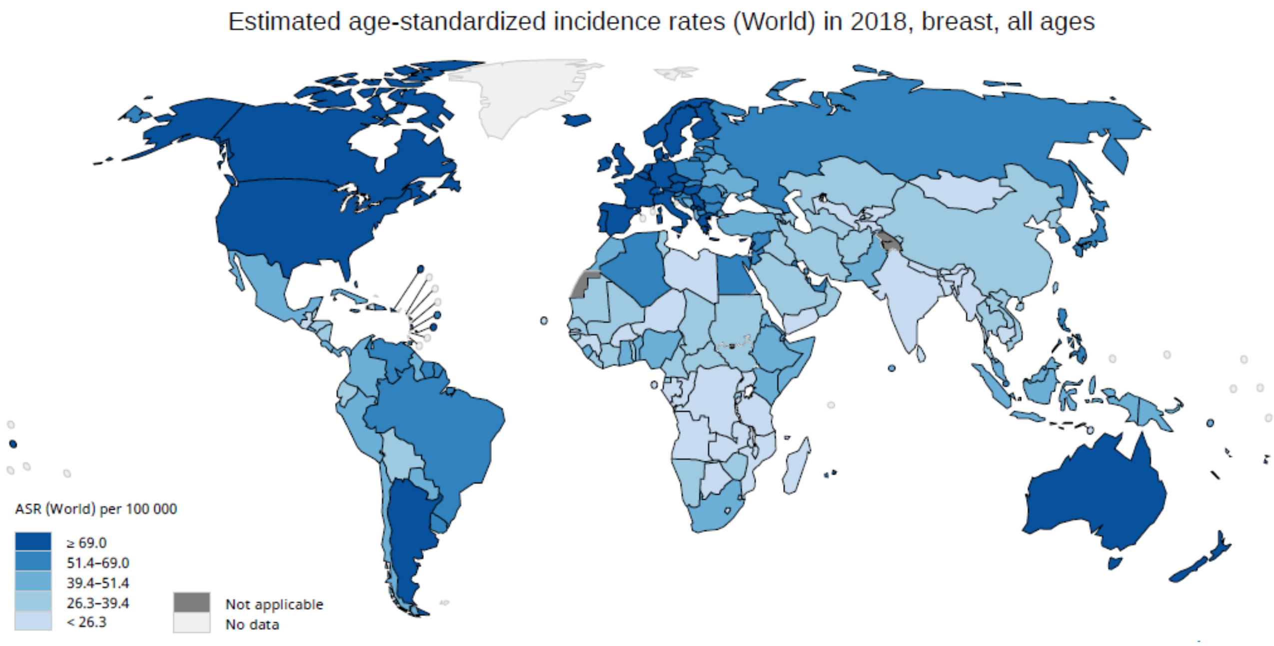

Figure 25: Patterns of distribution of breast cancer incidence worldwide (modified from WHO/IARC data retrieved from <http://globocan.iarc.fr/>, last access on 18 April 2018) [41].

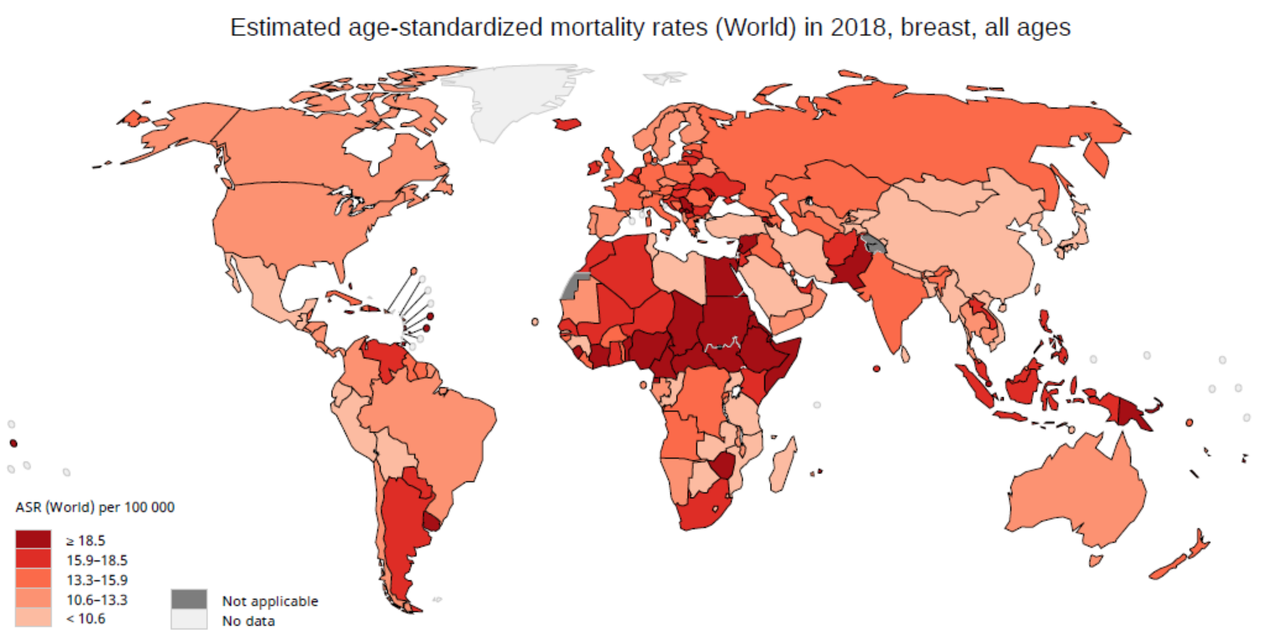

Figure 26: Patterns of distribution of breast cancer Mortality worldwide (modified from WHO/IARC data retrieved from <http://globocan.iarc.fr/>, last access on 18 April 2018) [41].

Risk factors related to life style: drinking alcohol has a high side effect in increasing the development of breast cancer with the amount of alcohol consumed. After menopause, having more fatty tissue or being obese can raise the estrogen levels and increase the chance of getting breast cancer. Physical exercises reduce the risk of getting breast cancer. Getting birth of the 1^{st} child over the age of 30 years will lead to the risk of breast cancer. Obesity is also another risk factor for breast cancer [46].

Behaviors that increase the risk of developing breast Cancer

Weight: Studies have found that the chance of getting breast cancer is higher in post-menopausal women who have not used menopausal hormone therapy and who are significantly overweight compared to peers who are of a healthy weight [44].

Smoking: Researchers at the American Cancer Society found an increased risk of breast cancer among women who smoke, especially those who started to smoke before having their first child [44].

Alcohol: The National Cancer Institute reported that over 100 studies document an increased risk of breast cancer associated with alcohol consumption [44].

Inactive lifestyle: Women who are physically inactive throughout their life may have an increased risk of breast cancer [44].

3.4 Tumor

A tumor is an abnormal lump or growth of cells. When the cells in the tumor are normal, it is benign. Something just went wrong and they overgrow and produce a lump. When the cells are abnormal and can grow uncontrollably, they are cancerous cells, and the tumor is malignant. To determine whether a tumor is benign or cancerous, a doctor can take a sample of the cells with a biopsy procedure. Then the biopsy is analyzed under a microscope by a pathologist, a doctor specializing in laboratory science [42].

3.4.1 Benign Tumors

A benign tumor is not a cancerous tumor. Unlike cancer tumors, a non-cancerous tumor is unable to spread throughout the body. Benign tumor cells grow only locally and cannot spread by invasion or metastasis. A benign tumor is less worrisome unless it is pressing on nearby tissues, nerves, or blood vessels and causing damage. Fibroids in the uterus or lipomas are examples of benign tumors. Benign tumors may need to be removed by surgery. They can grow very large, sometimes weighing pounds. They can be dangerous, such as when they occur in the brain and crowd the normal structures in the enclosed space of the skull. They can press on vital organs or block channels. Also, some types of benign tumors such as intestinal polyps are considered precancerous and are removed to prevent them becoming malignant. Benign tumors usually do not recur once removed, but if they do it is usually in the same place [47].

3.4.2 Malignant Tumors

Malignant tumor means the mass is cancerous. The word *malignant* is Latin for “badly born.” This type of tumor has the ability to multiply uncontrollably, to metastasize (spread) to various parts of the body and invade surrounding tissues. Malignant cells invade neighboring tissues, enter blood vessels, and metastasize to different sites. Malignant tumors are formed from abnormal cells that are highly unstable and travel via the blood stream, circulatory system, and lymphatic system. Malignant cells do not have chemical adhesion molecules to anchor them to the original growth site that benign tumors possess [42].

Breast cancer begins in the breast tissue and may spread to lymph nodes in the armpit if it is not caught early enough and treated. Once breast cancer has spread to the lymph nodes, the cancer cells can travel to other areas of the body, like the liver or bones. The breast cancer cells can then form tumors in those locations. A biopsy of these tumors might show characteristics of the original breast cancer tumor [47].

3.4.3 Difference between Benign and Malignant tumors

There are many important differences between benign and malignant tumors. Some of these include [37][43]:

- **Growth rate:** Malignant tumors may grow more rapidly than benign tumors, although there are slow-growing and fast-growing tumors in either category.
- **Ability to invade locally**: Malignant tumors may invade the tissue around them. One of the most prominent hallmarks of cancer is penetration of the basal membrane that surrounds normal tissues.
- **Ability to spread at distance:** Malignant tumors may spread to other parts of the body using the bloodstream or the lymphatic system. Malignant tumors may also invade nearby tissues and send out fingers into them, while benign tumors don't. Benign tumors only grow in the place where they started.
- **Recurrence:** Benign tumors are easier to remove by surgery as they have clearer boundaries, and as a result, they are less likely to recur. If they do recur, it is only at the original site. Malignant tumors may spread. As a result, they are more likely to recur and may recur in other sites, such as breast cancer recurring in the lungs or bones.
- **Cellular appearance:** When a pathologist looks at tumor cells under a microscope, it is often obvious whether they are normal, benign cells or cancerous cells. Cancer cells often have abnormal chromosomes and DNA, making their nuclei larger and darker. They also often have different shapes than normal cells. However, sometimes the difference is subtle.

- **Systemic effects**: While there are some benign tumors that secrete hormones, such as benign pheochromocytomas, malignant tumors are more likely to do so. Malignant tumors can secrete substances that cause effects throughout the body, such as fatigue and weight loss. This is known as paraneoplastic syndrome.

3.4.4 Appearance of Breast Tumors on Ultrasound

Ultrasound can assess the morphology, orientation, internal structure and margins of lesions from multiple planes with high resolution both in dense glandular structures and predominantly fatty breasts. A breast ultrasound is a helpful test in distinguishing between solid and cystic masses. In looking at an ultrasound report, the term "hypoechoic" refers to an area on the study that appears darker, and means the area is solid [46]. The complicated structure of breast ultrasound images makes it difficult in segmentation of breast tumors due to the fact that it has low signal and affected by noise ratio [48]. Among the general criteria's for breast cancer detection with ultrasound, mean intensity, variance, standard deviation and entropy features are significant factors in classification of a lesion.

Mass Due to Cancer on Ultrasound

On ultrasound, a breast cancer tumor is often seen as a solid mass (hypoechoic) that has irregular borders, and may appear speculated. Other findings on ultrasound that suggest a mass is breast cancer include [22]:

- Non-parallel orientation (not parallel to the skin),
- A mass that is taller than it is wide,
- Acoustic shadowing,
- Microlobulation,
- Duct extension,
- A branch pattern,
- A mass within a cyst,
- Angular margins, which means an irregular or jagged appearance to the mass.

Mass Due to Benign Conditions on Ultrasound

With benign masses, a fluid filled cyst may be noted. Areas that are dark (solid) are usually uniform, oval in shape, have a clearly defined capsule, are parallel to the skin, and have three or fewer lobulation. If a cyst is suspected, needle aspiration of the cyst can often result in the cyst disappearing completely [49].

3.4.5 Appearance of Breast Tumors on MRI

A breast MRI can sometimes provide better distinction between masses due to cancer and those related to benign causes than a mammogram, especially in women who have dense breasts. During a breast MRI, a contrast agent is injected into the bloodstream. When this contrast "lights up" on the image, the region that lights up is said to be enhanced and appears brighter than the surrounding tissue [49].

Mass Due to Cancer on MRI

Cancerous masses on MRI differ both in general appearance and the length of time they appear (kinetics). On MRI, a cancerous mass often has irregular or speculated borders with internal septation that enhances. Rim enhancement (brightening) on the outside of the mass is also common. Cancerous tumors also often have rapid signal intensity. In layman's terms, this means that the areas that are cancerous light up rapidly from the contrast when the image is taken, but then wash out rapidly (turn less bright) rapidly as well [49].

Mass Due to Benign Conditions on MRI

On MRI, benign breast masses often have smooth borders or are lobulated. If enhancement of the mass is present, it is usually minimal or patchy. The rise in signal intensity is slow (the image becomes bright only very slowly), and doesn't wash out (it stays bright) [49].

3.4.6 Appearance of Breast Tumors on Biopsy Test

When a breast biopsy is done, tissue is sent to a pathologist to look at under a microscope (and special molecular studies are usually done as well). The pathologist will look at the size and shape of the cells as well as the arrangement of cells (this can be seen on a core biopsy or open biopsy but not on a needle biopsy specimen) [49].

Mass Due to Cancer on Biopsy Test

Under the microscope, breast cancer cells may appear similar to normal breast cells (well-differentiated) or very little like breast cancer cells (poorly differentiated) depending on the tumor grade. Cancer cells differ from normal cells in many ways. The cells may be arranged in clusters, and may be seen invading blood vessels or lymphatic vessels. The nucleus of cancer cells can be striking, with nuclei that are larger, irregular in shape, and stain darker with special dyes. There are also often extra nuclei (rather than just one) present [49].

Mass due to Benign Conditions on Biopsy Test

Benign breast cells may look identical to normal breast cells, or different, but non-cancerous depending on the condition [49].

3.5 Breast Ultrasound Imaging

The use of ultrasound imaging in breast examination is first proposed by Wild and Neal [50]. Due to noninvasive modality of ultrasound, there are several properties inherent to ultrasound energy: i) Ultrasound has no known deleterious health effects, ii) Ultrasound obeys the laws of reflection and refraction, iii) Ultrasonic energy is reflected off of small objects, and iv) Ultrasound can be directed in a beam. For medical applications, these reasons are the basics of empowerment for ultrasound utilization [50].

Ultrasound is used in imaging abdominal organs, breast, heart, muscles, tendons, arteries and vein. It has no ionization effect and it can study the function of moving structures in real time [25].The real time moving images can be used to guide biopsy procedures and drainage. In short, ultrasound imaging is noninvasive, cost effective for diagnosis, harmless and it is one of the effective medical imaging technologies [25]. The detection rate of tumors in ultrasound images has been stated in different studies [25]. Breast ultrasound imaging is used to differentiate between solid tumors and fluid filled cysts. Lamps that are harder to see on mammogram are also evaluated using ultrasound and also it is used for screening women with dense breasts since mammography doesn’t report well results [25]. Ultrasound imaging is safe, has low acquisition time, is portable, inexpensive, noninvasive and it doesn’t have any known cumulative side effects [25]. Use of ultrasound reduces unnecessary biopsy by 40% and increase overall cancer detection by 17% [12].

Breast ultrasound doesn’t detect certain signs of cancer and it is not used for routine breast cancer screening. Breast ultrasound is used to evaluate breast abnormalities that are found during screening mammography. The ultrasound image has low resolution and low contrast, blurry edges between various organs and speckle noise. Hence, ultrasound diagnosis highly depends on doctor’s personal experience and expertise [50].

Ultrasound imaging of the breast uses sound wave to produce images of internal structure of the breast. Breast ultrasound imaging is used to distinguish between solid tumors and fluid filled cysts. It is also useful for screening of women with dense breast. Figure 27 depicts how imaging of the breast is performed on an ultrasound device.

Figure 27: Breast imaging of ultrasound in action [50].

3.6 Breast Mammography

Digital mammography is an effective universal technique used to decrease breast cancer mortality. Mammography screening results in a highly significant decrease in breast cancer-specific mortality [51]. Mammography is an imaging device which is used to view the changes in breast tissues by applying a low dose x-ray which is around 30Kvp. Mammogram is used for screening, detection and diagnosis of breast cancers. A typical breast cancer identified on a mammogram is shown in Figure 28.Through identification of characteristics masses or micro calcification, screening mammography detects small tumors with dimensions less than 1cm. Mammogram can early screen breast cancers before lump is developed or when it is small. American cancer society and American college of radiology recommend screening mammography for women above age of 40 [46].

Tiny minerals deposited within the breast tissue which appear as white spots on mammogram are called calcifications. There are two types of calcifications: micro and macro calcifications. Macro calcifications are bigger calcium deposits due to changes caused by aging of breast arteries, old injuries or inflammations. Such do not need to be checked by biopsy and they are related to non-cancerous conditions. 1 out of 10 women under 50, and half of women over 50 have macro calcifications. Micro calcifications are tiny specks of calcium in the breast. Radiologists judge changes due to cancer by looking the shape and layout of micro calcifications. Micro calcifications are seen by biopsy if suspicious look and patterns exists [46].

Masses also called lumps or tumors are areas that look abnormal and they can be many types like cysts (non-cancerous fluid-filled sacs) and noncancerous solid tumors (such as fibro adenomas), but they may also be a sign of cancer. Cysts do not need to be checked by biopsy because they are not cancerous [44].

For early screening of breast cancers, mammography is often the only screening tool. Mammography do not detect all kinds of breast cancers because some breast lesions and abnormalities are not visible and it is difficult for interpretation. Also when using mammography, the health risk of patients and radiologists increase with the ionizing radiation [12]. There is high rate of false positives in mammography which causes a lot of unnecessary biopsies. In women with dense tissue with a lot of ducts, glands, fibrous tissue, and less fat, breast cancer detection of mammography is less effective.

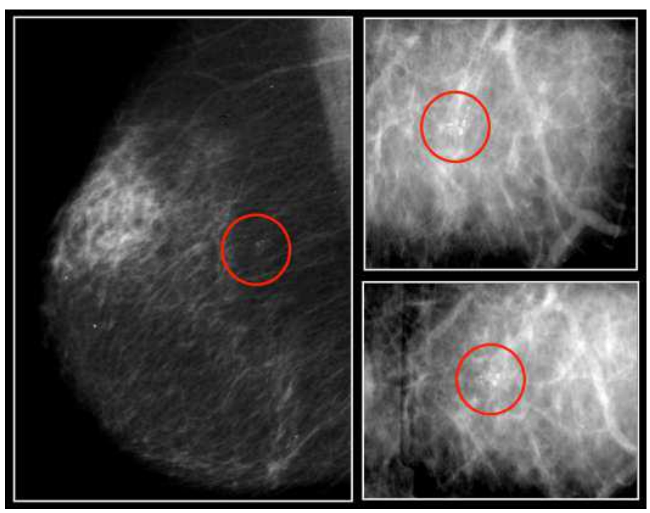

Figure 28: Breast cancer detected by screening mammography in a 52 year old woman. Red circles indicate micro calcifications. Images in the right panel represent enlarged details of the same area in two different projections [44].

3.7 Breast MRI

Magnetic resonance imaging (MRI) is an imaging technique used primarily in medical settings to produce high quality images of the soft tissues of the human body. MRI imaging defines the extent of malignant tissue and uses needle biopsy technique. American cancer society recommends also MRI for screening women at high risk of breast cancer [12].

MRI has a number of morphologic sequences to evaluate breast tissue density and morphological changes and to assess the condition of the skin, armpits and edges of the pectoral muscle. Breast MRI has the ability to detect malignancy that is clinically and mammographically occult [11]. MRI might find a new lesion in breast cancer patients who have been diagnosed. It was reported that MRI made 69 additional findings in 99 patients with breast cancer; of these, 51 findings were true positives, including 16 larger single lesions, 18 cases of multi-focality,7 cases of multi-centricity, 3 cases of contralateral lesions and 5 cases of lymph node involvement [11]. Many studies have reported that breast MRI is a promising method for screening young women at high risk for breast cancer [11][51].

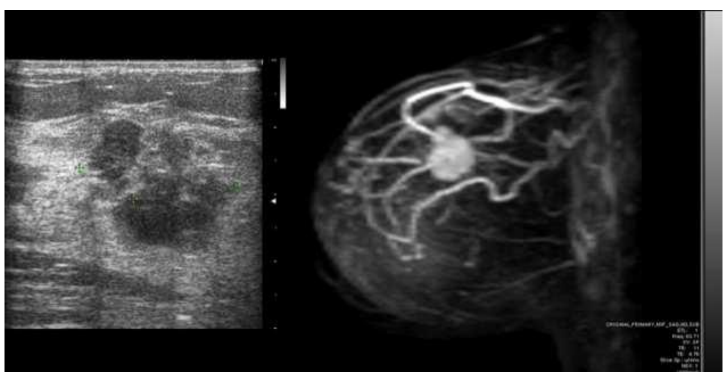

Figure 29: Breast cancer screening of a 40 year old woman: (left) using ultrasound showing a mass with irregular margins in the upper inner quadrant of the left breast, and (right) MRI with gadolinium contrast showing the mass has ductal-type contrast enhancement suggesting breast cancer (confirmed by needle core biopsy as infiltrating ductal carcinoma [44].

MRI utilizes magnetic fields to provide detailed cross sectional images of tissue structures and excellent soft tissue contrast. Contrast between tissues in the breast (fat, lesions, glandular tissue, etc.) depends on the mobility and magnetic environment of hydrogen atoms in fat and water that contribute to the measured signal that determines the brightness of tissues in the image. In the breast, this results in images showing predominantly fat and parenchyma, lesions, if they are present. A paramagnetic small molecular gadolium based contrast agent is injected intravenously to provide reliable detection of lesions and cancers. Thus, contrast enhanced MRI has been shown to have sensitivity for detecting breast cancer in high risk symptomatic and asymptomatic women, although reports of specificity have been more variable [22].

MRI is used as supplementary tool with ultrasound or mammography for breast screening. MRI scanning takes more time and costs more to perform scanning than ultrasound machine. Person with implant or metallic object is not supposed to take MRI exam. For pregnant women it is not recommended in that it has side effects on the fetus. It is difficult to distinguish between cancer and benign breast masses (such as fibroadenosis) in MRI. For screening women with high risk of breast cancer, MRI is very important. MRI is also important in identifying how large the cancer is and whether it involves underlying muscles. MRI identifies early breast cancer in women with dense breast and is used to assess tumor locations, determine the spread of cancer which is detected by ultrasound or mammography in the chest wall [51].

3.8 Beast Ultrasound Image Processing

There are various techniques reported in the literature for use in effective analysis of breast ultrasound images. The different techniques have their own merits and demerits. In one of the previous studies, Bikesh Kumar Singh studied the application of adaptive gradient descent (AGD) backpropagation for classification of breast tumors in ultrasound images based on variable learning rate and the technique offered classification accuracy of 84.6% [52]. The major drawback of the AGD algorithm is its time complexity. In another study, Guo et al. proposed a comparative study on ultrasound imaging technologies for breast cancer detection and concluded that fusion of ultrasound with other modalities could be an important tool for management of breast abnormalities [43]. Xian et al. also developed automatic breast ultrasound image segmentation tool and analyzed the performance [53]. The study showed that the performance of the segmentation tool degrades when considering images having large variations in quality as well as the number of artifacts involved and it was vital to develop a tool that is invariant to image settings.

Iesmantas Alzbutas, presented a conventional capsule network scheme for classification of breast cancer images that offered a classification accuracy of 84% [54]. Cheng et al. developed an automatic breast cancer detection and classification scheme using CAD technique and concluded that CAD has advantages over human classifiers since it is fast, stable, accurate, objective and consistent [55].

Walia Wakar used decision tree algorithm for classification of breast cancers (using 50 datasets) [56] while Osmanovic et al. investigated machine learning techniques for classification of breast cancers and concluded that artificial neural network (ANN) has acceptable level of accuracy for classification of breast cancers [57]. In another study, A. Vadivel et al. proposed a CAD system for detection and classification of breast tumors where fuzzy rules were framed using trapezoidal fuzzy membership functions for the shape classification of masses into different morphologies including round, oval, lobular and irregular [18].

One interesting technique used for effective analysis of ultrasound images relies on integral transforms. In this regards various real and complex valued transforms are available including the standard Fourier transform, Hartley transform, Gabor transform and wavelets. There are numerous resources available in the literature describing these integral transforms and their applications in different aspects of science. For 2D signals that do not show much spatial variation, say in terms of statistics, spatial frequency and the like, the use of the Fourier transform and its variants might be adequate. However, for 2D signals (images in our case) that show great spatial variation, like medical images, spatially localized integral transforms like wavelets are more informative [58]. The next chapter discusses one important integral transform that makes use of the wavelet theory known by the name Stockwell (S) transform. The chapter compares the S transform with that of wavelets and explains its typical advantages. A new methodology is later developed based on the S transform for use in effective analysis of breast ultrasound images.

Chapter 4

Proposed Scheme for Breast Cancer Detection and Classification Based on Ultrasound Image Processing

4.1 Data Set

The breast cancer data set was taken from research image database [59]. The proposed methodology was implemented on a MATLAB2015 platform. A total of 80 breast ultrasound images with 40 benign and 40 malignant tumors were used and the performance of the proposed algorithm in detecting and segmenting the tumors was verified against the available ground truth information, which was delineations by physicians. Unfortunately, the dataset didn't include control subject (normal cases). A priori to segmenting the tumors, first for each ultrasound image, in order to select the region of interest (ROI), the position of the mass was roughly located at the center of the original breast ultrasound image and then the image was cropped to the size of 128×128 pixels.

The proposed methodology primarily targets extraction of dominant imaging features based on the Stockwell (S) integral transform for use in accurate classification of breast mases in to benign and malignant. The different stages involved in the development of the proposed breast cancer detection system in this thesis have been explained below. Overall flowchart of the proposed methodology has been shown in Figure 30.

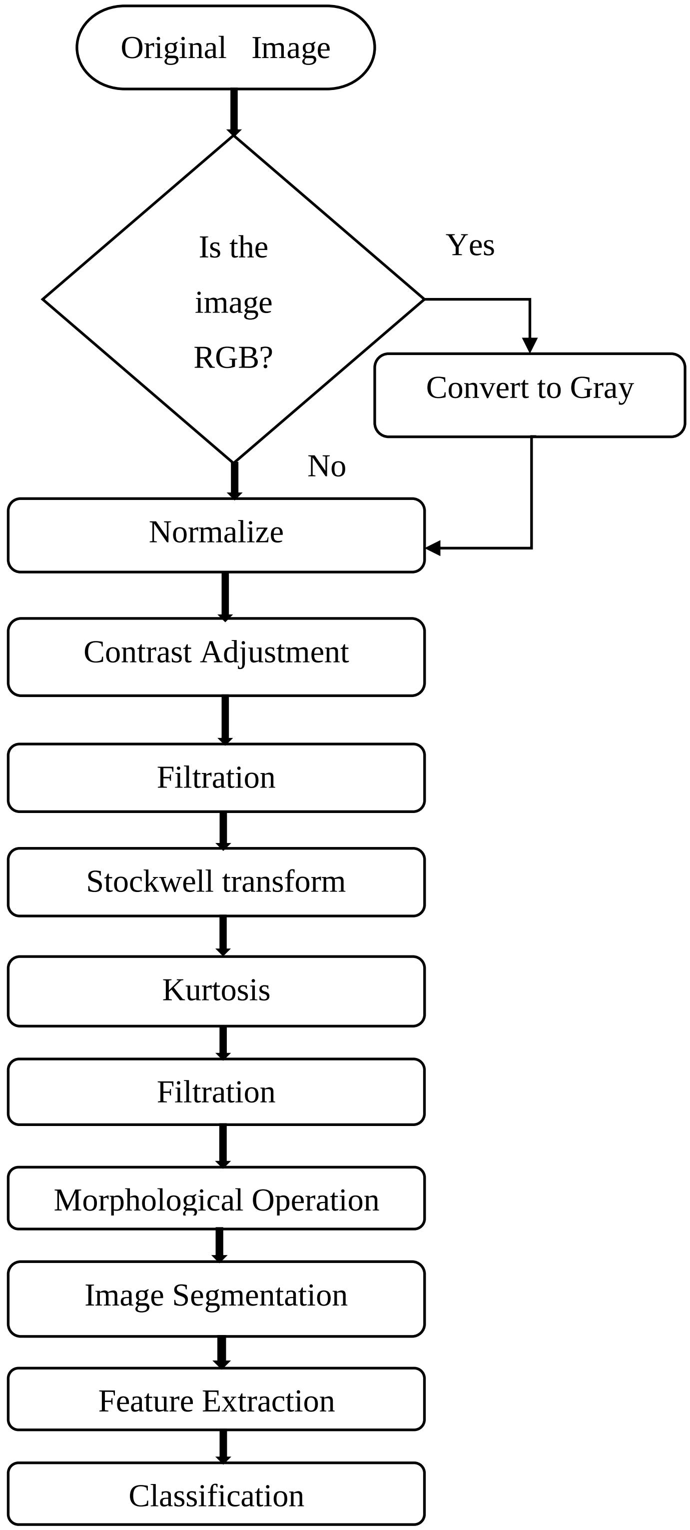

Figure 30: Flow diagram showing overall methodology of proposed technique.

4.2 Preprocessing

4.2.1 Filtering

Median Filter: The median filter is a nonlinear digital filtering technique which is used to remove noise. It is a smoothing filter often used for removal of impulse noise in ultrasound images. It is very widely used in digital image processing because, under certain conditions, it preserves edges while removing noise [21].When it is applied to grayscale images, the median filter is a neighborhood brightness ranking algorithm that works by first placing the brightness values of the pixels from each neighborhood in ascending order in which the median value of this ordered sequence is then selected as the representative brightness value for that neighborhood. Each pixel of the filtered image is expressed as the median brightness value of its corresponding neighborhood in the original image [21].

A major advantage of the median filter over linear filters is that the median filter can eliminate the effect of input noise values with extremely large magnitudes. The median filter does not create new unrealistic pixel values when the filter straddles an edge and because of this, the median filter is better in preserving edges [21]. For an $M\ x\ N$ size input noisy image $I\ (x, y)$, the median filter is given by:

$$f(x, y) = median\{I(i, j)|(i, j) \in W\} \qquad \text{(Eq. 4.1)}$$

where $f(x, y)$ is the filtered image, 'i' and 'j' are the row and column coordinates respectively for $i = 1{:}m$ and $j = 1{:}n$ while 'W' is a translating window of size '$m \times n$' centered at the point (x, y) where the operation takes place and median represents the median value over the window [60]. The Matlab 'medfilt2' function implements the median filtering with a given window width.

Wiener Filter: The objective of wiener filter is to filter out noise that has corrupted a signal based on statistical approach. Wiener filter (a type of linear filter) is applied to an image adaptively, tailoring itself to the local image variance. Where the local image variance is large, wiener filter performs little smoothing [60]. It performs smoothing when the variance is small. Wiener filter is often used for speckle noise removal which is often common in ultrasound images.

Wiener filter is based on both global statistics (mean, variance, and higher order moments of entire image) and local statistics (mean, variance, and higher order moments of kernel) and is given by:

$$f(x,y) = \mu + \frac{\sigma_W^2}{\sigma_W^2 + \sigma^2}\left(W_{xy} - \mu\right) \qquad \text{(Eq. 4.2)}$$

where $f(x,y)$ denotes the filtered image, μ is the local mean, σ_W^2 is the local variance, W_{xy} is the intensity of the (x,y)'th pixel in the translating window W defined in Eq. 4.1, and σ^2 is the global variance [61]. The Wiener filter is mostly implemented in the spectral/frequency domain and requires knowledge of power spectrum of the noise involved and power spectrum of the noise free image. The power spectrum of the noise could be somehow modeled if the type of noise is known a priori. However, the power spectrum of the noise free (un-degraded) image is seldom known and wiener filter applies some kind of approximation to it. The Matlab 'wiener2' function implements the Wiener filtering with a given window width.

4.2.2 Image Enhancement

Contrast Adjustment: Contrast adjustment remaps image intensity values to the full display range of the data type. A grayscale image with good contrast has sharp differences between black and white. Increasing contrast, you are making the blacks darker and the whites brighter. Hence, in order to increase the difference between the lesion and background in our ultrasound images, the image contrast is adjusted. This intern will increase the image dynamic range (the number of distinct gray values in the image). This can be done by using a linear stretching function as given in Eq. 4.3.

$$\sqrt{\frac{1}{MN}\sum_{i=0}^{N-1}\sum_{j=0}^{M-1}\left(g_{ij} - \bar{g}\right)^2}, \qquad \text{(Eq. 4.3)}$$

where intensities g_{ij} are the i-th j-ith element of the two-dimensional image g of size M by N. $\bar{g}$ is the mean intensity of all pixel values in the image.

The Stockwell (S) Transform: The Stockwell transform (ST) is an integral transform that makes use of the wavelet theory to effectively analyze non-stationary signals, signals with temporally varying frequency characteristics. For images, the 2D ST offers joint space-wave number/spatial frequency information. It is similar to the short time Fourier (Gabor) transform but uses variable resolution. Compared to the wavelet transform, which is widely used in many aspects of signal and image processing, the S transform has several superior properties that make it a better tool: as opposed to the wavelet transform, there is a direct relationship between the ST and the natural Fourier transform, it is less noisy and keeps the so called absolutely referenced phase information [62][63].The S transform is defined based on a scalable localizing Gaussian window and supplies frequency dependent resolution.

For a 2-D continuous domain function $g(x, y)$, the 2-D ST with a 2-D Gaussian envelope is defined as [64]:

$$S(x, y, K_x, K_y) = \int_{-\infty}^{\infty}\int_{-\infty}^{\infty} g(x', y') w(x, y, K_x, K_y) e^{-i2\pi(K_x x' + K_y y')} dx'\, dy' \qquad \text{(Eq. 4.4)}$$

where x and y are translation variables while K_x and K_y are the spatial frequencies, in the x and y directions respectively, and the Gaussian window function $w(x, y, K_x, K_y)$ is choosen as:

$$w(x, y, K_x, K_y) = \frac{|K_x||K_y|}{2\pi} e^{-\frac{(x'-x)^2 K_x^2 + (y'-y)^2 K_y^2}{2}} \qquad \text{(Eq. 4.5)}$$

The S-transform is generally complex valued and assumes two attributes: amplitude and phase. The power spectrum is computed as the square of the amplitude.

Kurtosis: Kurtosis is a measure of whether the data are flat or peaked relative to a normal distribution. Data with high kurtosis tend to have a distinct peak near the mean, have heavy tails and declining rapidly while data with low kurtosis tend to have flat top near the mean [65]. For an image g of size $m\ x\ n$ with W containing all pixels, the kurtosis f is computed using the formula given in Eq. 4.6. Figure 30 presents a breast ultrasound image and a map showing kurtosis features computed from the power spectrum of the 2D ST. what appeared as dark region on the kurtosis map is a confirmed breast cancer.

$$f(x,y) = \frac{\frac{1}{mn-1}\sum_{(i,j)\epsilon W}\left(\frac{1}{mn-1}\sum_{(i,j)\epsilon W}\left(g(i,j) - \frac{1}{mn-1}\sum_{(i,j)\epsilon W} g(i,j)\right)\right)^4}{\left(\frac{1}{mn-1}\sum_{(i,j)\epsilon W}\left(\frac{1}{mn-1}\sum_{(i,j)\epsilon W}\left(g(i,j) - \frac{1}{mn-1}\sum_{(i,j)\epsilon W} g(i,j)\right)\right)^2\right)^2} \quad \text{(Eq. 4.6)}$$

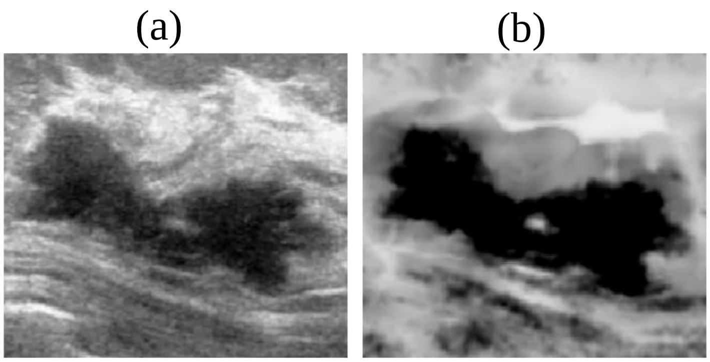

Figure 31: Application of ST and Kurtosis (a) Original image (b) Enhanced image after processing original image through ST and Kurtosis.

4.2.3 Morphological Operations

Morphology in context of image processing means description of shape and structure of objects in an image [66]. When images are processed for enhancement and while performing some operations like thresholding, there is more chance for distortion of the image due to noise. As a result, imperfections exist in the structure of the image. The main goal of morphological operations is to eliminate such imperfections that mainly affect the shape and textures that exist in images. Hence, morphological operations are useful in image segmentation as the process directly deals with shape extraction in an image [67][66]. The fundamental morphological operations are *erosion* and *dilation*. The others, *opening* and *closing*, which are used in this thesis study are dependent on these two basic operations.

Dilation: The dilation operation makes an object to grow by size. Formally, the dilation of set A by B is defined by [66]:

$$A \oplus B = \left\{ z | \left(\hat{B} \right)_z \cap A \neq \emptyset \right\} \qquad \text{(Eq. 4.7)}$$

If set B is reflected about its origin and shifted by z, then the dilation of A by B is the set of all displacements z such that $\hat{B} = \{-b: b \in B\}$ is the reflection of B and A have at least one common element. Dilation simply adds pixels to the boundary elements.

Erosion: The erosion operation causes object to lose its size. The erosion of set A by set B is defined by [66]:

$$A \ominus B = \left\{ z | \left(\hat{B} \right)_z \subseteq A \right\} \qquad \text{(Eq. 4.8)}$$

The erosion of image A by structuring element B is the set of all points z such that the structuring element B translated by z is a subset of the image. This operation results in loss of boundary pixels of the object.

Opening: The opening of an image is a combinational operation of erosion and dilation. The opening of an image A by structuring element B is defined as [66]:

$$A \circ B = (A \ominus B) \oplus B \qquad \text{(Eq. 4.9)}$$

The above definition states that the opening operation is nothing but the erosion of an image and the resultant is dilated. The boundary of the opened image is the points in the structuring element B that reaches the extreme points of the boundary of A as B is rolled around inside of this boundary. The union set operation is used to find the points of the opened image. The opening operator is demonstrates on Figure 31b. As can be seen on the figure, opening operation smooths contour of an object and also eliminates minor protrusions, thing present out from an object.

Closing: The closing of an image is also a combinational operation of erosion and dilation. It differs from the opening operation in the sense of order of occurrence of erosion and dilation operation. The closing of an image A by structuring element B is defined as [66]:

$$A \cdot B = (A \oplus B) \ominus B \qquad \text{(Eq. 4.10)}$$

The relation between erosion and dilation with closing is given in the above mathematical statement. It shows that closing operation is the dilation of an image A by the structuring element B and the resultant is eroded with the same structuring element. The boundary of the closed image is the points in the structuring element B that reaches the extreme points of the boundary of A when B is rolled over A around outside of its boundary. Figure 31 demonstrates closing and opening operators. As can be seen on the Figure 31c, closing operation in general blends narrow breaks and thin gaps. As a result, it eliminates small holes and fills gaps in the objects boundaries.

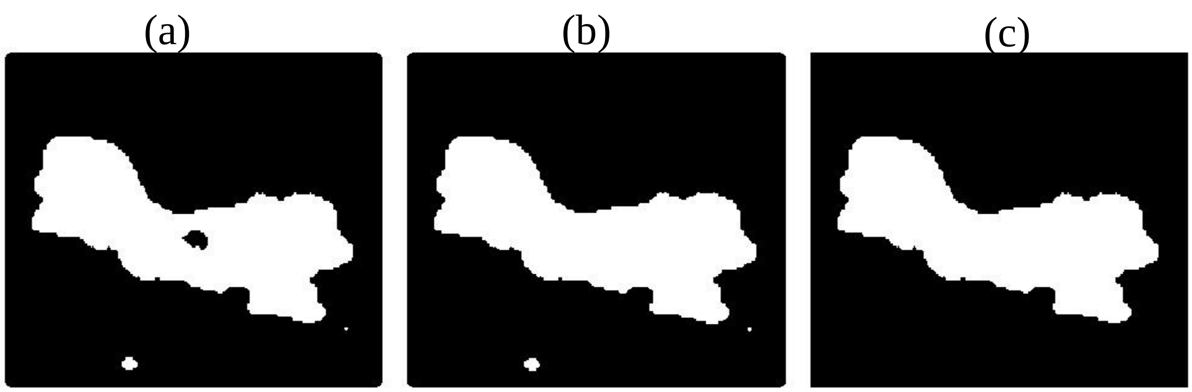

Figure 32: Morphological operations: (a) A preprocessed image after thresholding, (b) Opening operation to fill gaps, (c) Closing operation to remove small objects outside the region of interest.

4.3 Segmentation

Segmentation is the process of dividing an image into non-overlapping regions, such that each region is homogeneous but the union of any two neighboring regions is inhomogeneous [6]. Thus, segmentation separates an image into its component parts or objects.

After preprocessing the input image, segmentation of the target region is done. Image segmentation when applied on breast images extracts the region of interest (ROI) thereby separating breast masses from the surrounding tissue. Conventional segmentation methods like thresholding method, canny filter, region growing etc. have been used previously in many different applications [67]. In this thesis study, because of its superiority to other conventional techniques, canny filter has been used for edge-based image segmentation after pre-processed images are converted into black and white color and morphological operation is applied. The next sub-section explains the canny edge detection scheme in detail.

4.3.1 Canny Edge Detection

Edge detection is a fundamental tool for image segmentation. Edge detection methods transform original images into edge images. For gray scale (non-color) images, edge detection benefits from the local changes of grey tones in the image [55]. It is a fundamental process that detects and outlines an object and its boundaries among other objects and the background in the image. Edges typically occur on the boundary between two sections.

There are many edge detection techniques proposed in the literature for use in image segmentation. Those techniques include Roberts's edge detection, Sobel edge detection, Prewitt edge detection, canny edge detection and the like. Of these edge detection techniques, canny edge detection is used in this thesis [55]. Canny edge detection is one of the standard and multi-step algorithm that can detect edges with noise suppressed at the same time. Canny involves the following major steps:

I. Smoothing

Image smoothing is the first step in canny edge detection. It is blurring of an image to suppress its noise content. Images are smoothed using a low pass Gaussian filter by convolving the image $I(i,j)$ with a 2D Gaussian function $G(i,j)$ resulting in a filtered image $f(i,j)$ as shown in Eq. 4.11.

$$f(x,y) = G_\sigma(i,j) * I(i,j)$$

where

(Eq. 4.11)

$$G_\sigma = \frac{1}{\sqrt{2\pi\sigma^2}} exp\left(\frac{i^2 + j^2}{2\sigma^2}\right)$$

II. Compute gradient

The edges should be marked where the gradients of the image have large magnitudes. First the gradient operator is applied on the smoothen image from step I to compute the edge strength (edge magnitude) and direction. The Canny algorithm basically finds edges where the grayscale intensity of the image changes the most. These areas are found by determining gradients of the image. Gradients at each pixel in the smoothed image are determined by applying what is known as the Sobel-operator (kernel). First step is to approximate the gradient in the x and y direction respectively by applying the kernels shown in Eq. 4.12.

$$G_x = \begin{bmatrix} -1 & 0 & 1 \\ -2 & 0 & 2 \\ -1 & 0 & 1 \end{bmatrix} * I(i,j)$$

(Eq. 4.12)

$$G_y = \begin{bmatrix} 1 & 2 & 1 \\ 0 & 0 & 0 \\ -1 & -2 & -1 \end{bmatrix} * I(i,j)$$

Where $*$ denotes the 2 dimensional signal processing convolution operation. The gradient magnitudes (also known as the edge strengths) can then be determined as a Euclidean distance measure by applying the law of Pythagoras as shown in Eq. 4.13.

$$|G| = \sqrt{G_x^2 + G_y^2} \qquad \text{(Eq. 4.13)}$$

$$|G| \approx |G_x| + |G_y|$$

Where: G_x and G_y are the gradients in the x- and y-directions respectively.

Figure 32 presents a breast ultrasound image (left) which has been preprocessed and smoothed following the procedures presented earlier. The right-hand side shows the respective edge strength computed from the gradient image using Eq. 4.13.

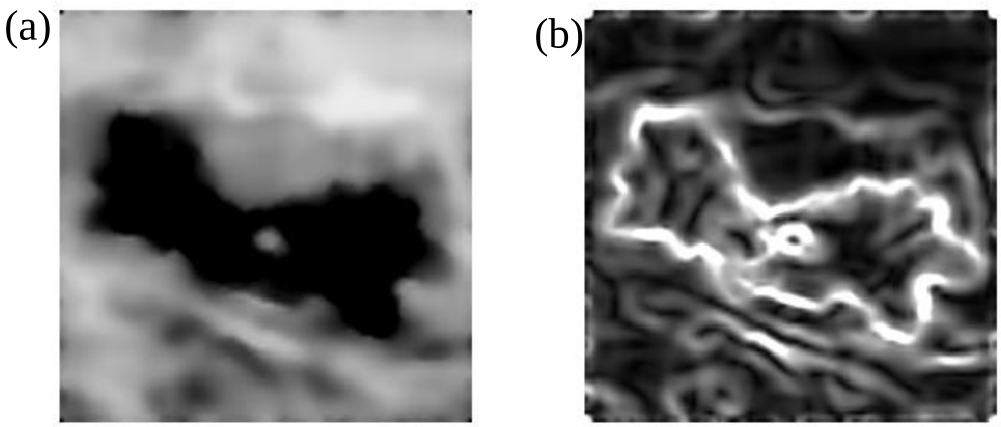

Figure 33: The preprocessed smoothed image (left) and the gradient magnitude (right).

It is obvious from Figure 32 that the gradient magnitude indicates the edges quite clearly. However, the edges are typically broad and thus do not indicate exactly where the edges are. To make it possible to determine these, the direction of the edges must be determined and stored as shown in Eq. 4.14.

$$\theta = arctan\left(\frac{|G_y|}{|G_x|}\right) \qquad \text{(Eq. 4.14)}$$

III. Non-maximum suppression

The purpose of this step is to convert the blurred edges in the image of the gradient magnitudes to sharp edges. It is done by preserving all local maxima in the gradient image, and deleting everything else. Thus, if a pixel is not a maximum, it is suppressed or set to 0.

IV. Double Thresholding

The Canny edge detection algorithm uses double thresholding. Edge pixels stronger than the high threshold are marked as strong; edge pixels weaker than the low threshold are suppressed and edge pixels between the two thresholds are marked as weak. This known as hysteresis thresholding. The application of non-maximum suppression and hysteresis thresholding is illustrated in Figure 33.

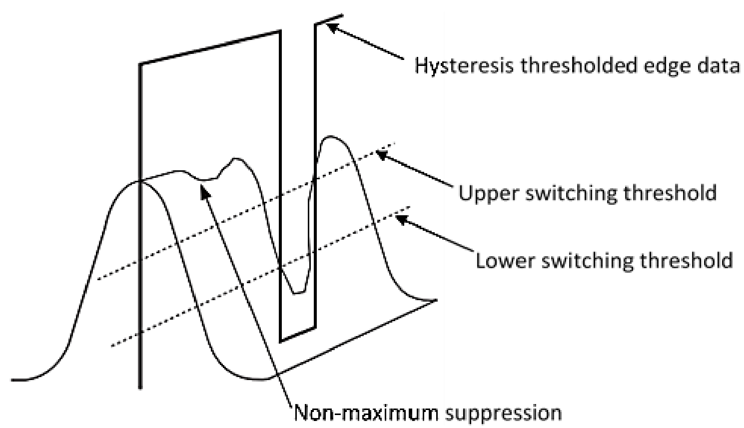

Figure 34: Action of non-maximum suppression and hysteresis thresholding.

V. Edge tracking by hysteresis

Strong edges are interpreted as certain edges, and can immediately be included in the final edge image. Weak edges are included if and only if they are connected to strong edges. The overall edge detection process can be seen in Figure 34.

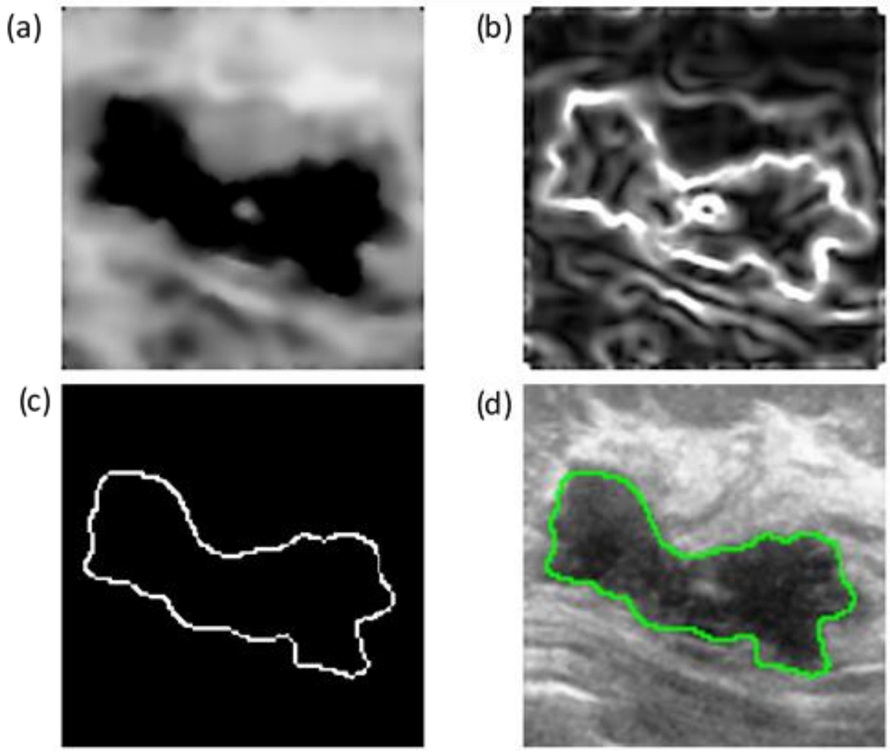

Figure 35: The overall edged detection process using canny edge detection is shown: (a) Preprocessed image, (b) Processed gradient imaged (c) After the application of thresholding and edge tracking by hysteresis, (d) Segmented region of interest.

4.4 Feature Extraction

This step is to find a feature set of breast cancer lesions that can accurately distinguish lesion from nonlesion or benign from malignant. Features are extracted from the segmented images to classify them into benign and malignant ones. According to [7], mass can be classified into benign or malignant depending on the features of the ultrasound image. This mainly includes texture features like mean, variance, standard deviation, entropy and contrast [52].

If we assume $g(i,j)$ is the $(i,j)'$ th entry of size $W = m \times n$ ultrasound image matrix, and then the statistical measure image becomes $I(x,y)$.

Mean: shows average intensity level of an image.

$$I(x,y) = \frac{1}{mn} \sum_{(i,j)\epsilon W} g(i,j) \qquad \text{(Eq. 4.15)}$$

Variance: used to find how each pixel varies from the neighboring pixel and measures how far a set of numbers is spread out.

$$I(x,y) = \frac{1}{mn-1} \sum_{(i,j)\epsilon W} \left(g(i,j) - \frac{1}{mn-1} \sum_{(i,j)\epsilon W} g(i,j) \right)^2 \qquad \text{(Eq. 4.16)}$$

Standard deviation: used to characterize the amount of 2D dispersion around the mean.

$$I(x,y) = \sqrt{\frac{1}{mn-1} \sum_{(i,j)\epsilon W} \left(g(i,j) - \frac{1}{mn-1} \sum_{(i,j)\epsilon W} g(i,j) \right)^2} \qquad \text{(Eq. 4.17)}$$

Entropy: measures the uniformity/variability of an image histogram.

$$I(x,y) = - \sum_{(i,j)\epsilon W} g(i,j) \left(\log\left(g(i,j) \right) \right) \qquad \text{(Eq. 4.18)}$$

Correlation: Correlation is measurement of the similarity between two signals/sequences.

$$g_x(i) = \sum_{j=1}^{n} g(i,j), \qquad g_y(j) = \sum_{i=1}^{n} g(i,j) \qquad \text{(Eq. 4.19)}$$

Where n is the number of distinct gray levels of the image.

$$I(x,y) = \frac{\sum_{(i,j)\epsilon W} (i \times j) g(i,j) - \mu_x \mu_y}{\sigma_x \sigma_y} \qquad \text{(Eq. 4.20)}$$

Where μx, μy, σ_x and σ_y are the means and standard deviations of g_x and g_y.

Contrast: Contrast is the difference in luminance or color that makes an object distinguishable from other objects within the same field of view.

$$I(x,y) = \sum_{k=0}^{L-1} k^2 \times \sum_{(i,j)\epsilon W} \delta(|i-j|,k)g(i,j)$$

(Eq. 4.21)

Where, L is the number of distinct gray levels of the image and

$$\delta(x,y) = \begin{cases} 1, & x = y \\ 0, & x \neq y \end{cases}$$

In this thesis, ones the above features are computed, the following matrices were derived to create the final feature sets for use in further classification:

- Mean ;
- Variance;
- Standard deviation;
- Entropy and
- Contrast.

4.5 Classification

After the features have been extracted and selected, they are input into a classifier to categorize the images into benign/malignant classes. Different methods have been used in the literature for doing so [7]. One commonly used classifier is artificial neural network (ANN) and of the various neural network models, the most widely accepted one is back propagation neural network [BPNN] [52]. It provides the needed weight adjustments in the backward sweep [55]. Its performance can be improved by using variable learning rate during the training process i.e. instead of using constant learning rate, adaptive learning rate can be employed.

Cross Validation: In the training of neural network, *k*-fold cross validation is used to split the data into train and test which makes the test result more meaningful and reliable. In *k*-fold cross-validation, the whole original data is randomly partitioned into *k* equal size sub samples. Of the *k* sub samples, in each case, each of the k sub samples is used as validation data and the remaining is used for training. The cross-validation process is then repeated k times (the folds) [68]. Based on this method, in this thesis 8 fold cross validation is used to train over 80 dataset.

The ANN in the current study was implemented on MATLAB-15, configured with five input neurons (number of attributes) and one output neuron (benign or malignant). Trial and error was used by changing three parameters: number of layers, number of neurons in hidden layers and transfer functions, to get better performance of different ANN architectures. The ANN within this study was configured with 20 of number neurons in first hidden layer and 1 in the second hidden layer. The transfer functions used were tansig for the first hidden layer and pureline for the second hidden layer. The structure of the ANN is shown in Figure 35. The trained networks were Feed Forward and 30 data sets of benign and malignant breast cases were used for training and 80 benign and malignant breast cases were used for testing and the trained ANN classifies the data to benign and malignant based on the training.

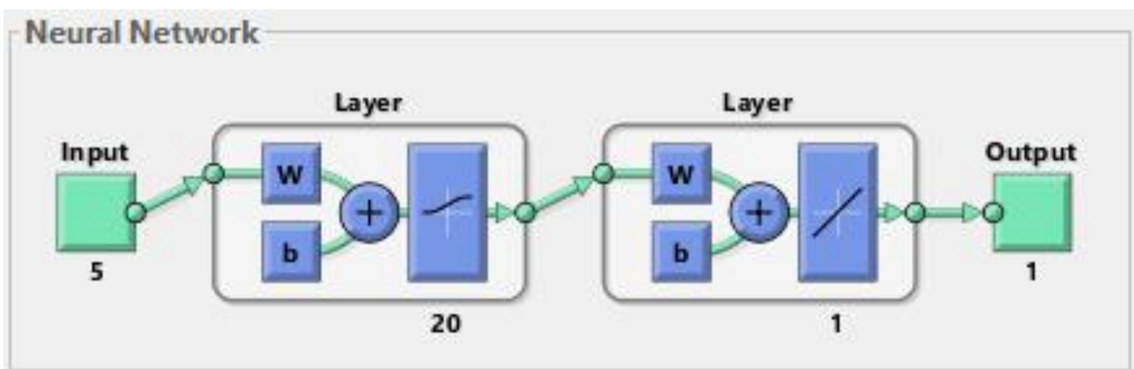

Figure 36: Architecture of ANN.

The accuracy of the classifier was measured by computing the overall accuracy measure shown in Eq. 4.22 by comparing it against available gold standards.

$$Accuracy = (TP + TN)/(TP + TN + FP + FN) \quad \text{(Eq. 4.22)}$$

where TP: true positives, TN: true negatives, FP: false positives and FN: false negatives.

4.6 Classification Performance

Other than the overall accuracy, the classification performance of the proposed scheme has been evaluated based on the following measures.

4.6.1 Decision Boundary

In classification problems, prediction of a particular class is involved among multiple classes. In other words, it can also be framed in a way that a particular instance (data-point) needs to be kept under a particular region (signifying the class) and needs to be separated from other regions. This separation from other regions can be visualized by a boundary known as decision boundary. This visualization of the decision boundary in feature space is done on a scatter plot where every point depicts a data-point of the data-set. The decision boundary separates the data-points into regions, which are actually the classes in which they belong [69].

Dimension Reduction Technique: The main goal of the dimensionality reduction techniques is to transform the data or features from a higher dimensional space to a lower dimensional space. Principal Component Analysis (PCA) is a linear transform that converts the data to a new coordinate system such that the first principal component (PC) lies on the coordinate that has the largest variance by projection of the data, the second PC lies on the coordinate with second largest variance, and so on [70]. PCA reduces the dimensionality of a data set consisting of a large number of interrelated variables, while retaining as much as possible of the variation present in the data set. This is achieved by transforming to a new set of variables, the principal components (PCs), which are uncorrelated, and which are ordered so that the first few retain most of the variation present in all of the original variables [71].So, dimension of the 5 computed features is reduced with the first three principal components in the decision boundary.

4.6.2 ROC

An ROC curve (receiver operating characteristic curve) is a graph showing the performance of a classification. A test with perfect discrimination (no overlap in the two distributions) has a ROC curve that passes through the upper left corner. Therefore, the closer the ROC curve is to the upper left corner, the higher the overall accuracy of the test [72][73].

4.6.3 AUC

Area under the ROC curve (AUC) measures the entire two-dimensional area underneath the entire ROC curve (think integral calculus) from (0, 0) to (1, 1). AUC provides an aggregate measure of performance across all possible classification. AUC ranges in value from 0 to 1. A model whose predictions are 100% wrong has an AUC value of 0.0; one whose predictions are 100% correct has an AUC of 1.0 [72][73].

4.6.4 Canberra Distance

This is used in order to measure how well the decision boundary separates two classified vectors. In our case, the Canberra distance is used to measure distance between classified benign and malignant points/pixels in vector space. The Canberra distance between two vectors U and V is given by

$$CB(U,V) = \sum_{i} \frac{|u_i - v_i|}{|u_i| + |v_i|}, \qquad \text{(Eq. 4.23)}$$

Where i runs from one to number of ultrasound image set in our case. The Canberra distance is believed to be a better metrics compared to the traditional distance matrices such as Euclidean and Mahalanobis distances [58][74].

Chapter 5

Results and Discussion

5.1 Preprocessing Results

An ultrasound image contains speckle noise which is random and granular in nature and that gives the ultrasound image its characteristic appearance. The speckle noise needs to be minimized for better segmentation which in turn improves the classification accuracy of ultrasound images [75]. Following the procedures explained in the previous Chapter, the ultrasound images were all first contrast enhanced and then filtered with median and wiener filters. Following this step, the complex 2D S transform is computed and the local power is calculated to create the power map. At each pixel position, the local power is calculated as the sum of square of the local amplitude spectrum computed over the spatial frequencies in the x and y directions. A second filtration (using median and wiener filters) was applied on the power map for further image enhancement. Figure 36 presents an example ultrasound image and its preprocessing results. The last image is the power map plotted using an HSV pseudo coloring scheme applied for the sake of visualization. The example clearly shows that the preprocessing stage could highlight breast lesions differentiating them from the background. Appendix A includes the Matlab code for the implementation of the preprocessing and segmentation procedures.

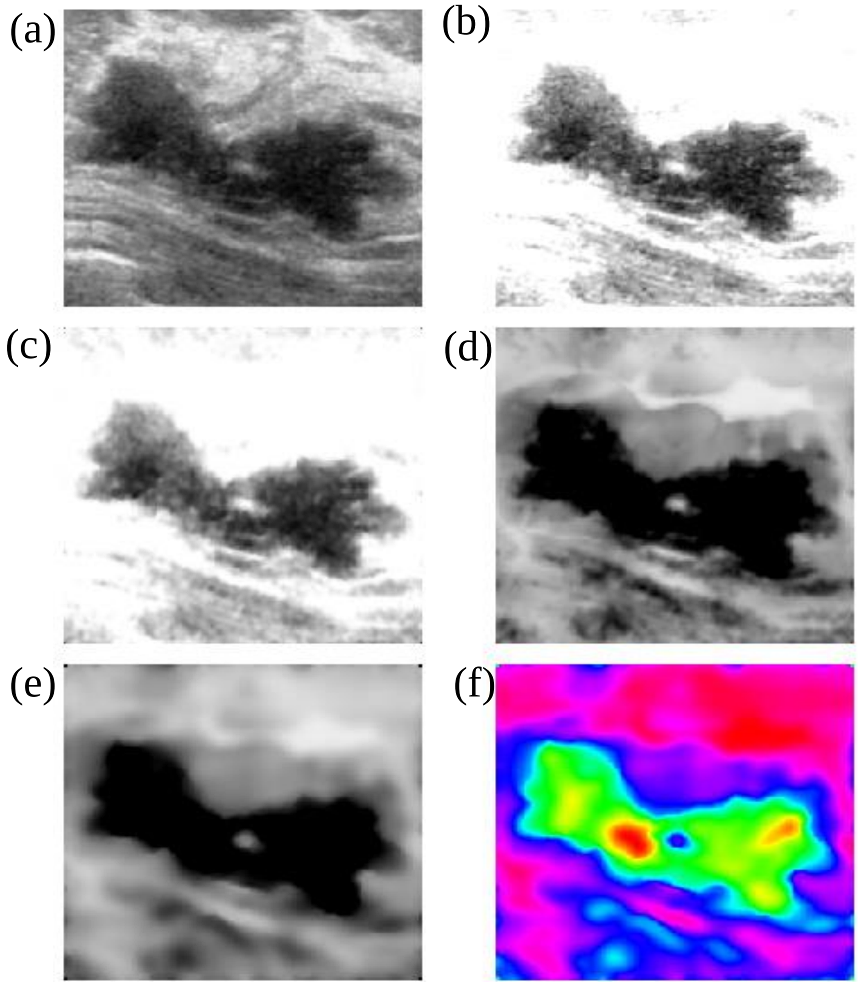

Figure 37: Preprocessing result: (a) Original image (b) Contrast enhanced (c) Filtered (d) Power map of the S transform of the filtered (e) Filtered power map (f) The power map in HSV pseudo coloring.

5.2 Segmentation Results

After preprocessing the input images, segmentation of the target region is done using the segmentation scheme explained in the previous Chapter which involves canny edge detection. Figure 37 shows a typical segmentation result presented here for demonstration. Figure 38 and Figure 39 present segmentation results for a typical malignant and one benign breast tumor cases respectively using the proposed segmentation scheme. Malignant tumors often have very irregular shapes while the shape of benign cases is relatively regular (rounded shape).

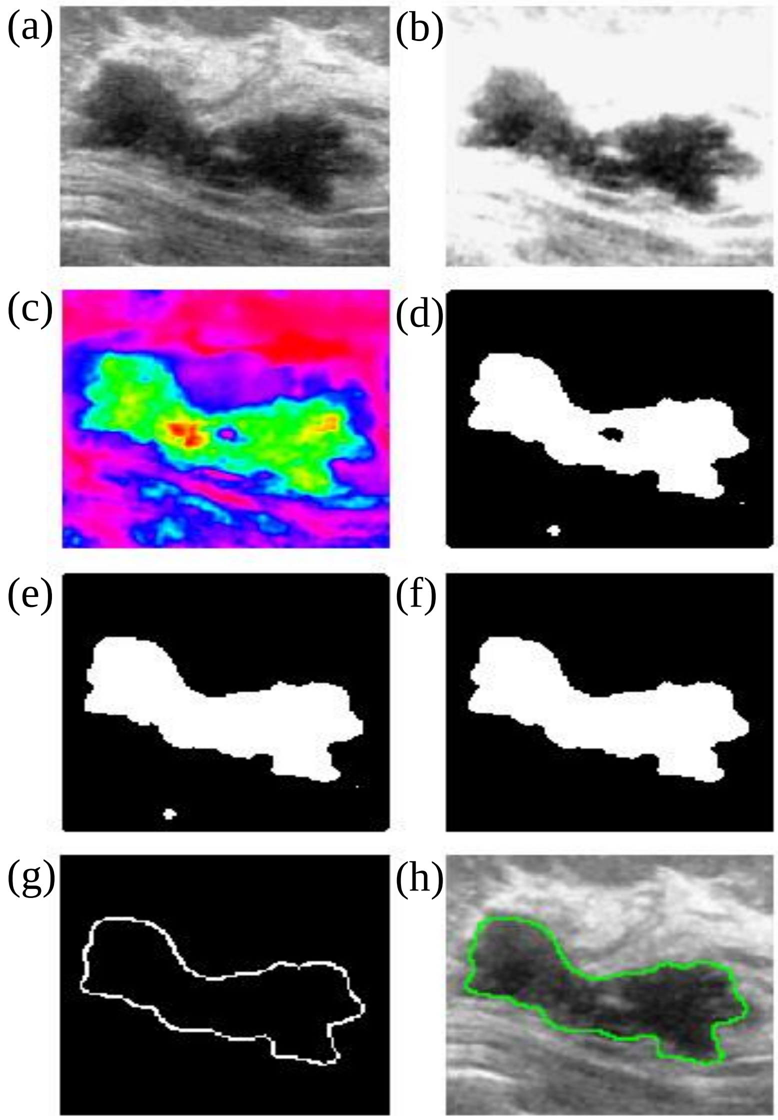

Figure 38: Overall steps of the image segmentation scheme: (a - c) are the preprocessing steps, (d - f) show the morphological image processing steps, (g) is the canny edge detection result while (h) is the segmented image.

5.2.1 Malignant Solid Mass Segmentation

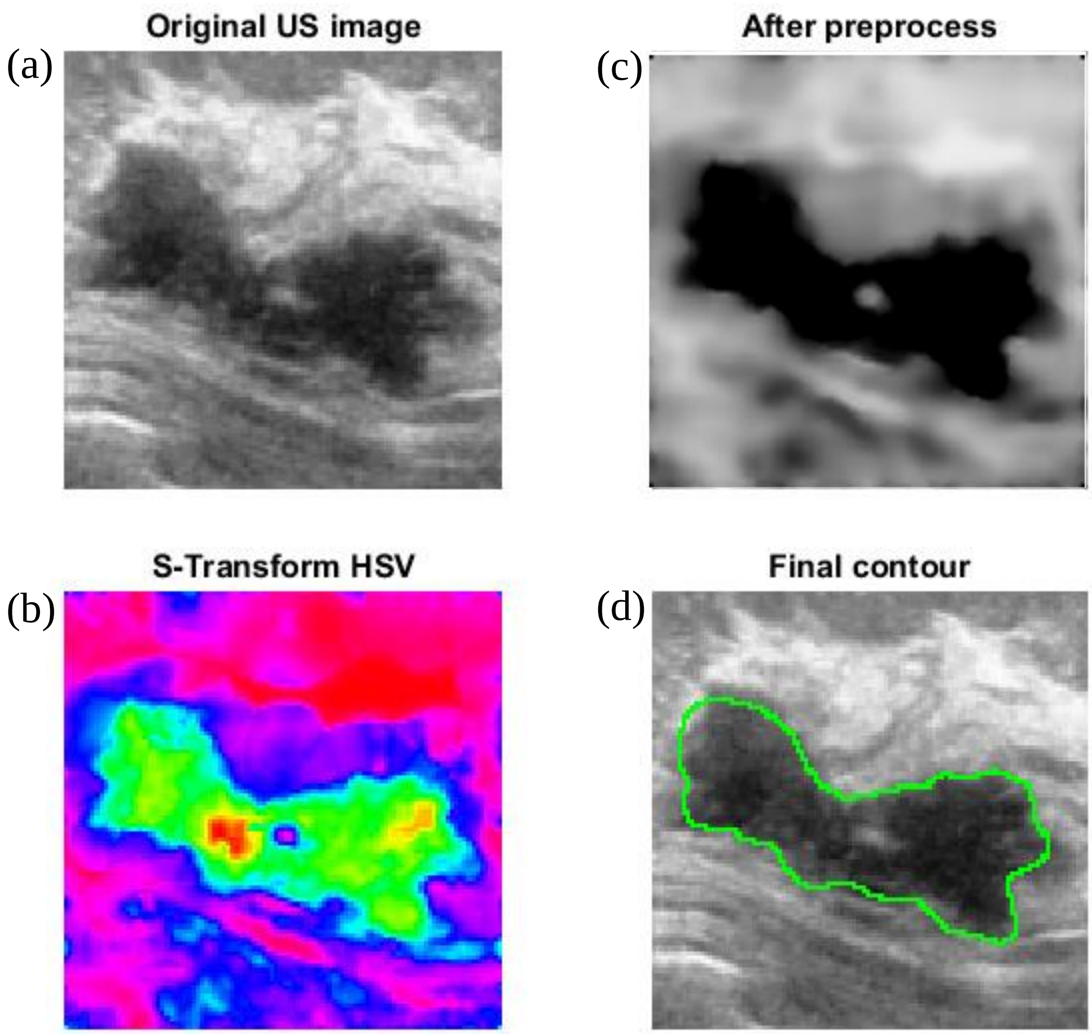

Figure 39: Segmentation of malignant ultrasound breast image.

5.2.2 Benign Solid Mass Segmentation

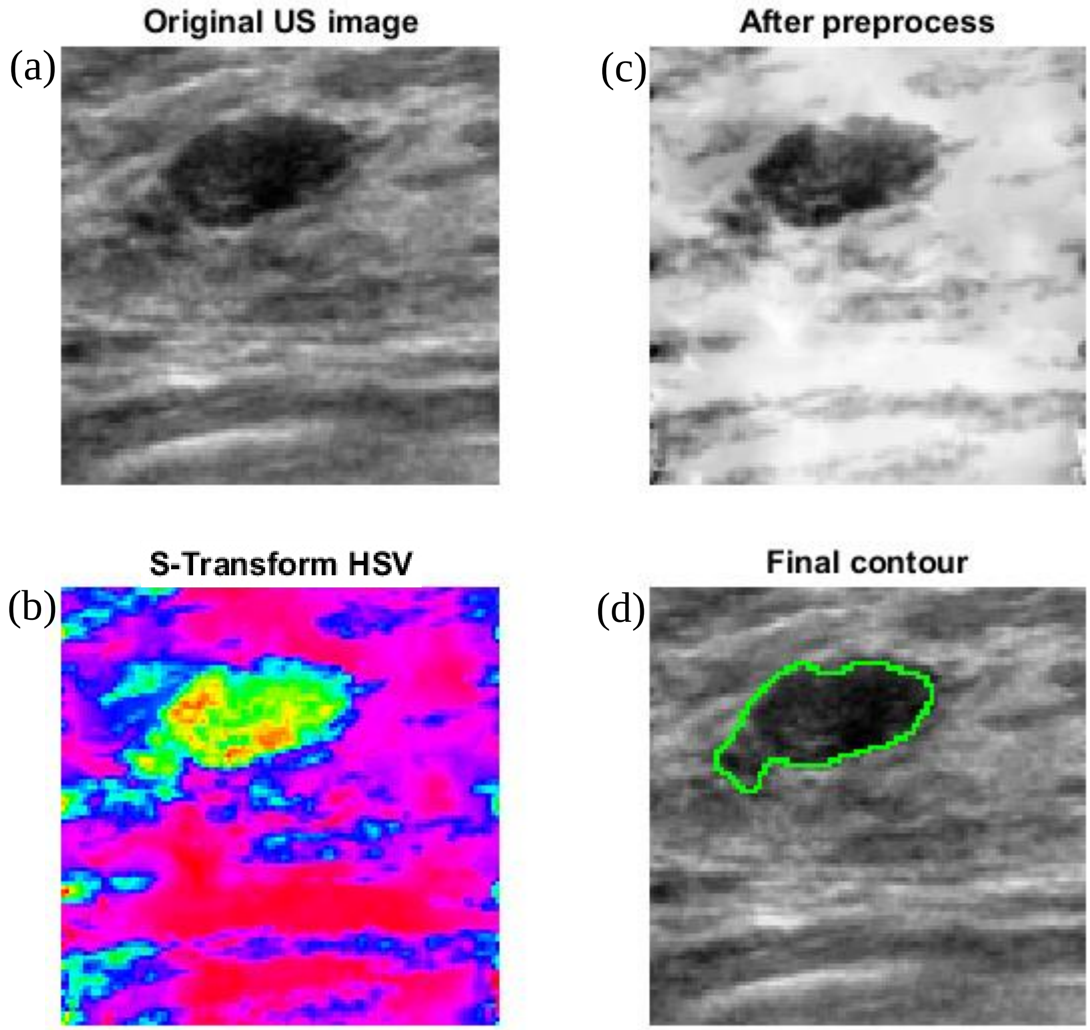

Figure 40: Segmentation of benign ultrasound breast image.

5.2.3 Segmentation Results versus Available Ground Truth

The ground truth is hand drawn by leading radiologist [59]. Qualitative comparisons were made between the segmentation results generated using the proposed segmentation algorithm and the available ground truth, which are delineations performed by an expert physician. Demonstrating examples are shown in Figure 40. Generally, the segmentation performance is better with benign cases compared to malignant cases the reason being benign regions have relatively more regular boundary with close to oval or round shapes while malignant ones are more irregular in shape.

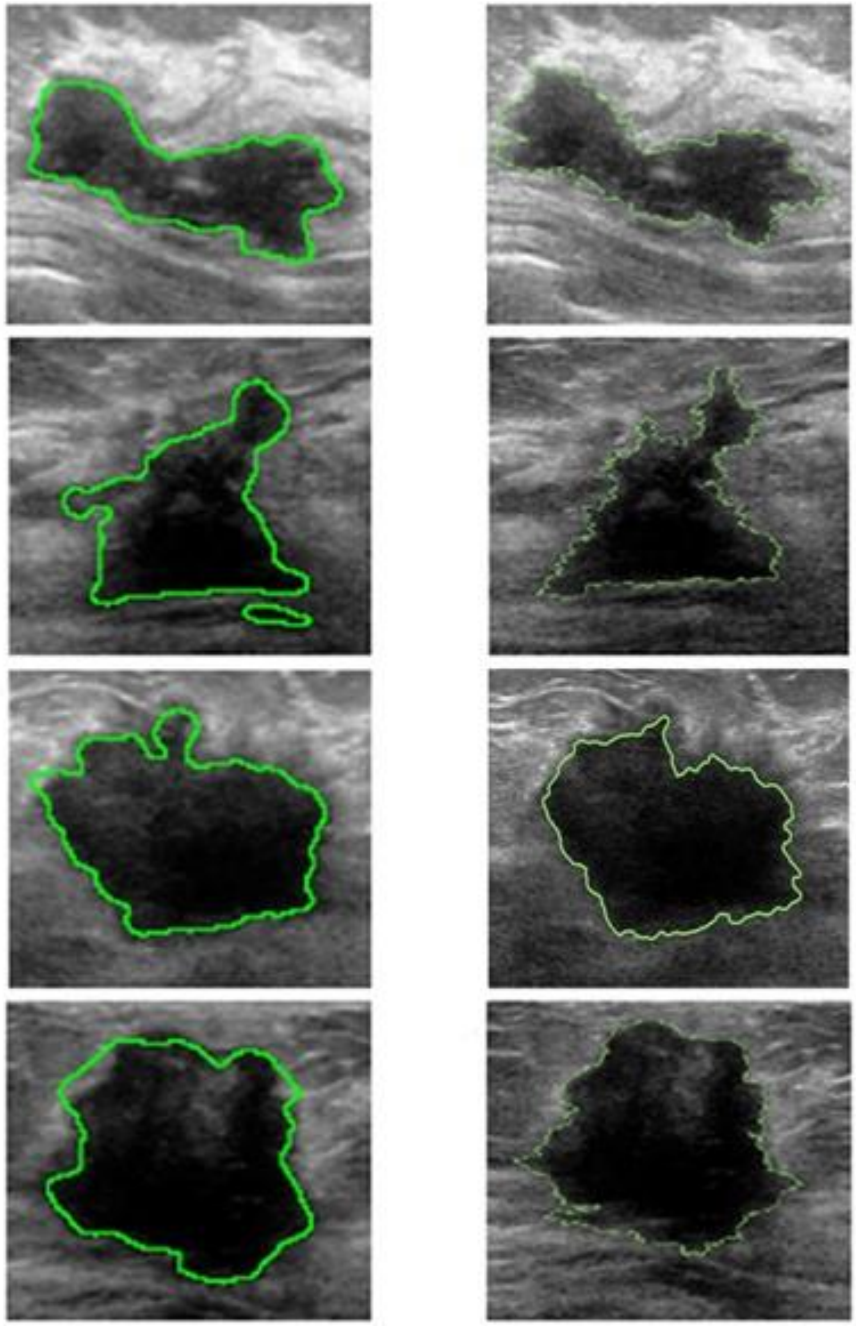

Figure 41: Comparison of some of the segmentation results (left) with available ground truth (right).

5.3 Feature Selection

Five features were computed (as explained in Chapter 4) and compared for their ability in uniquely quantifying breast lesions as malignant or benign. These features were mean intensity of ROI to background ratio, variance of ROI to background ratio, STD of ROI to background ratio, entropy ROI to background ratio and contrast of ROI to background ratio. Figure 42 presents these features computed for different malignant and benign breast tumor cases.

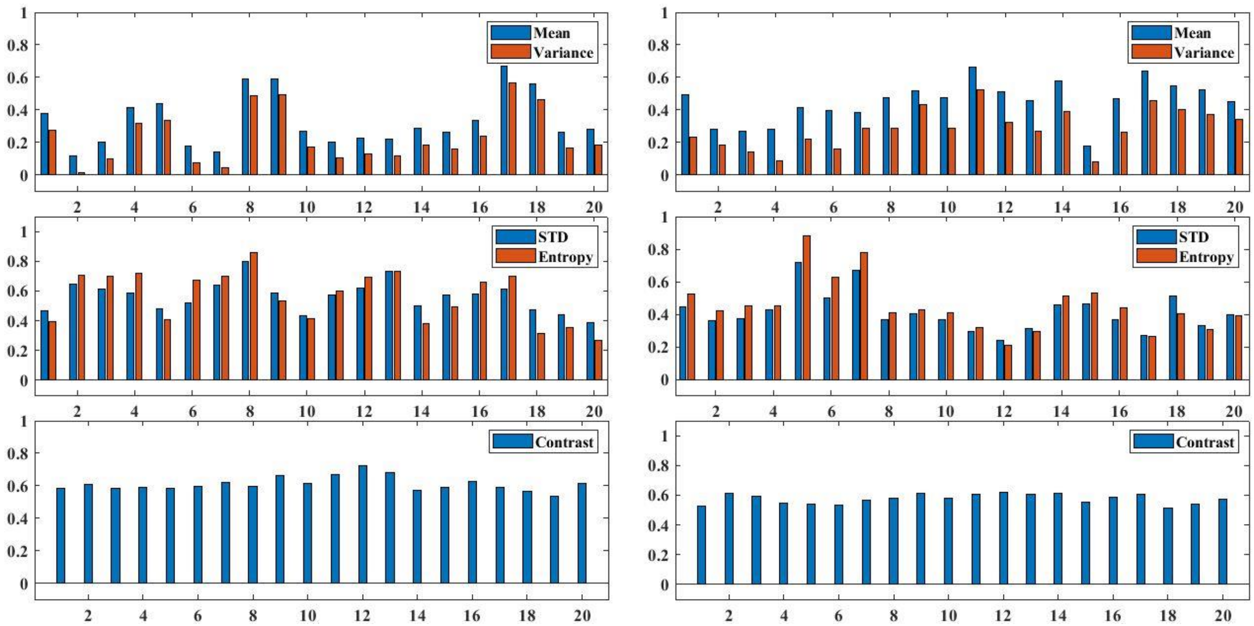

Figure 42: (a) to (f): mean intensity, variance, standard deviation, entropy and contrast features computed for malignant (left) and benign (right) cases.

5.3.1 Feature Comparison of Malignant vs Benign Cases

Figure 43 presents comparison between the five features computed for malignant and benign breast tumor cases considered and Figure 44 presents feature comparison with boxplot. Clearly, benign and malignant tumors show different feature values in all cases. However, from the results we could conclude that no single feature could be used for final classification of benign and malignant tumors. Artificial Neural Network (ANN) is used to find combination of features that could be used to derive a decision boundary to be used to correctly differentiate between malignant and benign tumors.

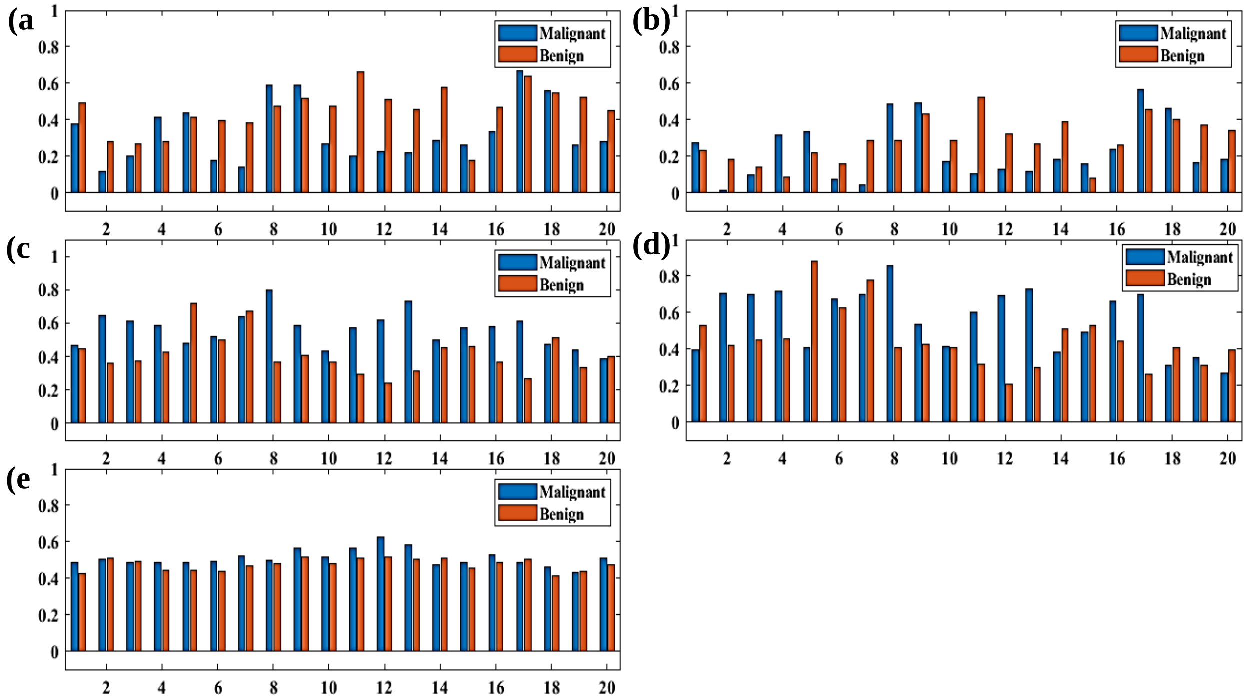

Figure 43: Comparison of malignant and benign features: (a) Mean intensity (b) Variance (C) Standard deviation (d) Entropy and (e) contrast. All features were normalized between 0 and 1.

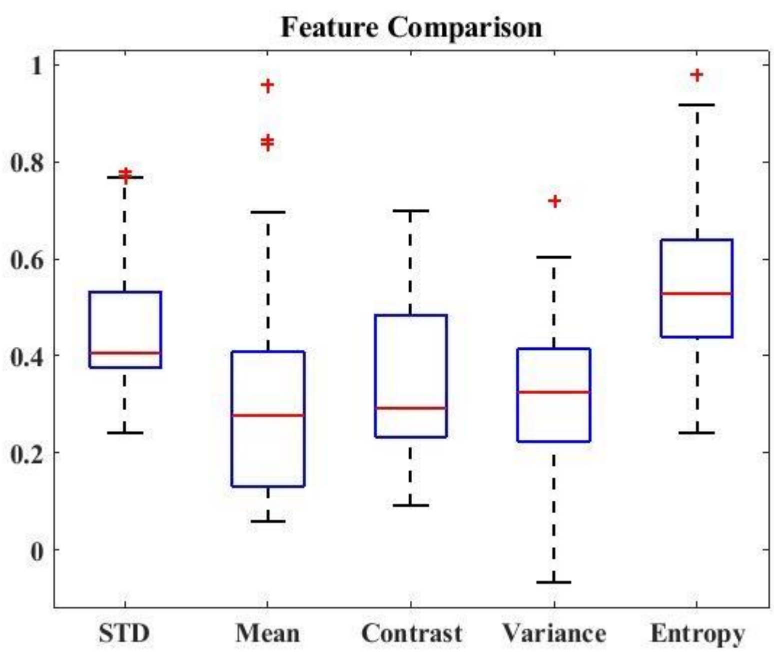

Figure 44: Feature Comparison with boxplot where the middle line of the box refers 'median' and + sign refers outlier.

5.4 Artificial Neural Network Results

Based on the five features extracted, the ultrasound images were categorized into benign and malignant cases using Artificial Neural Network (ANN). The ANN within this study was configured with five input neurons (number of attributes) and one output neuron (benign or malignant) with 20 neurons in the first hidden layer, 1 neuron in the second hidden layer. Training of the ANN was carried out with 30 malignant and benign cases and tested with 80 more data sets. The training and testing were carried out entirely on a Matlab platform (MATLAB15).

Table 3 presents the classification accuracy of each of the five features computed individually and compares it against the combination using ANN. Clearly individual features offered a classification accuracy which is much inferior to the ANN. The Entropy feature performed better than the other four features. (80% versus 50% average).

Table 3: Classification accuracy of different features.

No.	**Features**	**Detection Accuracy**
1	Mean	55%
2	Variance	30%
3	Standard deviation	65%
4	Entropy	80%
5	Contrast	50%
6	Combination of all five features (using ANN)	90%

Table 4: Classification result of datasets

Datasets	Correctly Classified	Incorrectly Classified
Benign	37	4
Malignant	34	6

5.5 Decision Boundary

Figure 43 presents the decision boundary created after the application of the ANN classifier. As shown in the Figure, the decision boundary separates the malignant 'Red' and the benign 'Green' data sets. However, there are few overlap data sets, which account for the error. Nevertheless, most of the data sets are clearly separated.

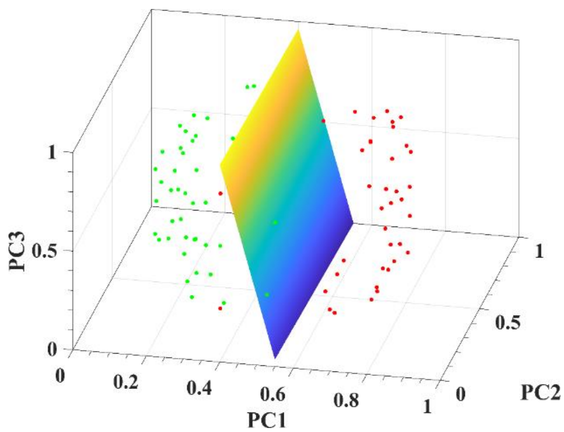

Figure 45: 3D decision boundary of ANN classification of the five computed features with the first three principal components. The 'Red' and 'Green' represent malignant and benign cases respectively.

5.6 ROC and AUC

In order to further quantify the classification performance of the proposed classification scheme, ROC curves were generated with the corresponding AUC values. Figure 44 presents such for the five features computed and the ANN combined features. The plots make it obvious that the ANN combined features out perform all the other five computed features showing its great promises. The ANN combined features offered the highest AUC value of 0.99 followed by the entropy feature which offered an AUC value of 0.85. The rest four features much smaller AUC values. A complete list of the overall accuracies as well as AUC values computed for the different features has been presented in Table 4 while Figure 45 presents a bar plot of the respective overall accuracies.

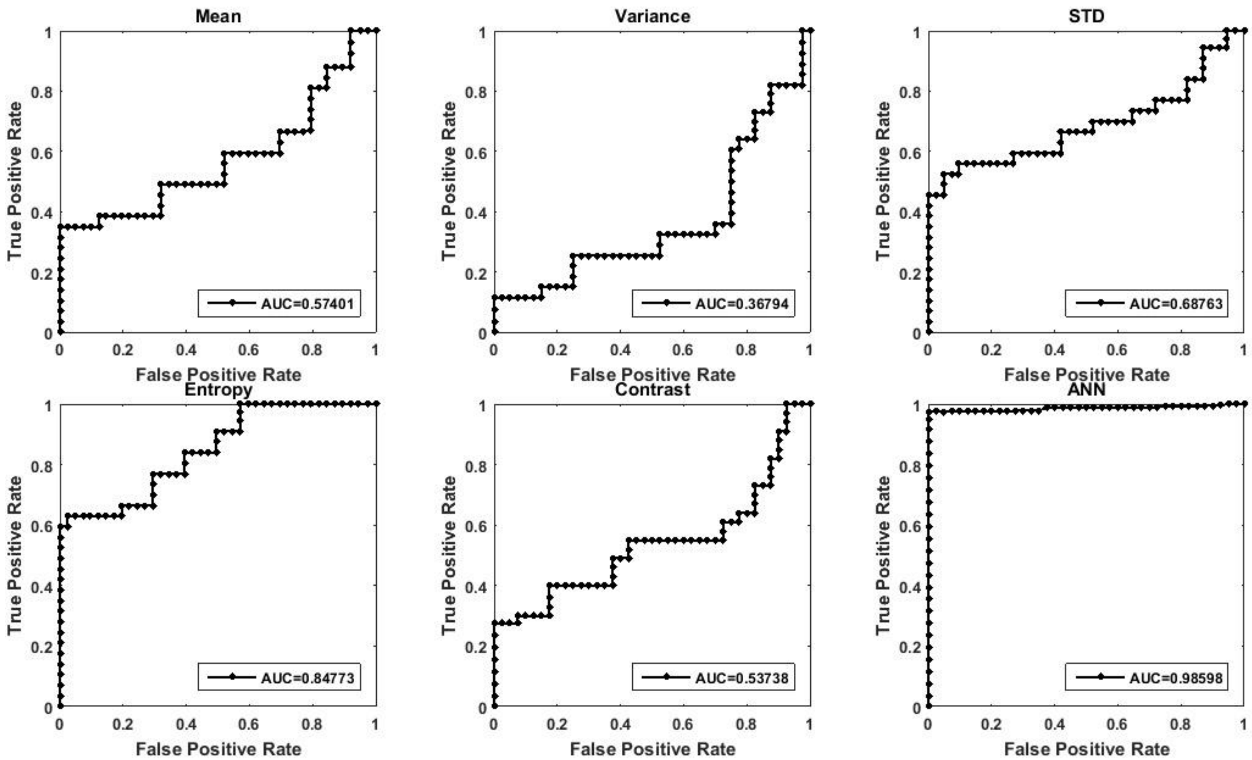

Figure 46: ROC curves plotted for different features computed showing their classification performance.

5.7 Canberra Distance

Canberra distance is computed using Equation 4.23 and the computed distances for all features has been summarized in Table 4.

Table 5: AUC values, maximum classification accuracies, and Canberra distances for different features.

No.	Features	AUC	Accuracy	Canberra Distance
1	Mean	0.57401	55%	10.1296
2	Variance	0.36794	30%	7.7785
3	Standard Deviation	0.68763	65%	11.4363
4	Entropy	0.84773	80%	12.1078
5	Contrast	0.53738	50%	9.0716
6	Combination of all five features (using ANN)	0.98598	90%	13.8407

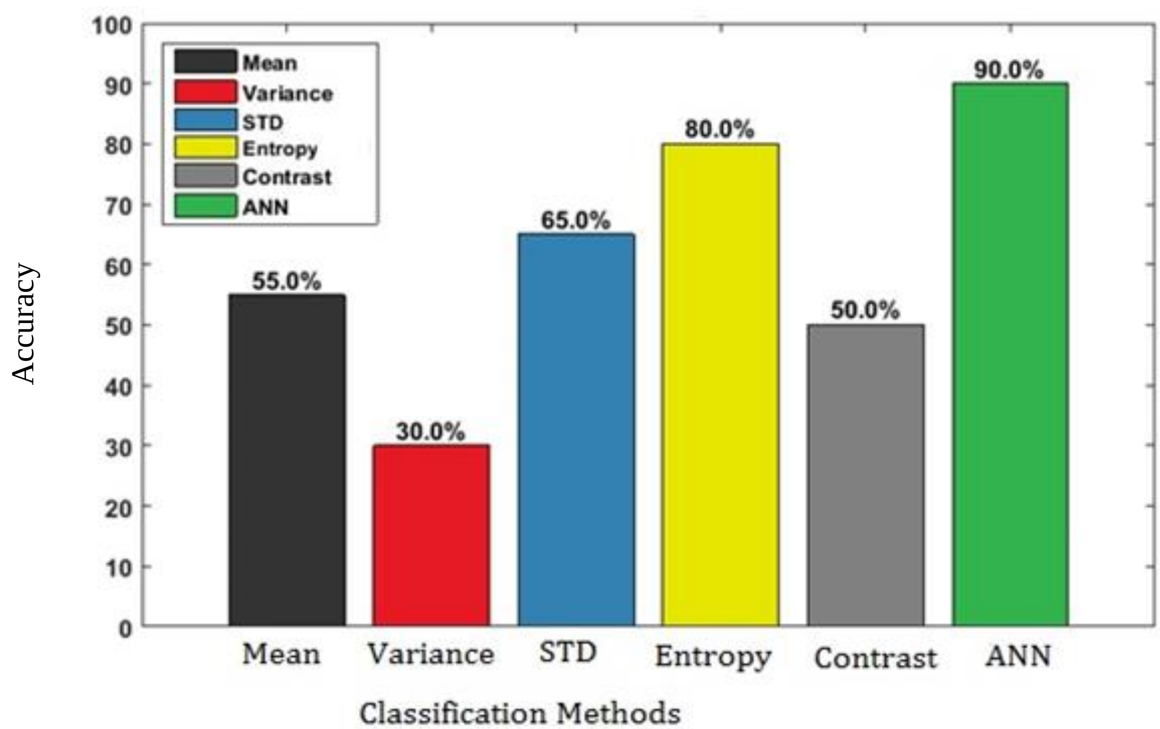

Figure 47: Comparison of performance accuracy by different features.

Chapter 6

Conclusion and Future Works

6.1 Conclusion

The main purpose of this thesis study was to extract useful features from breast ultrasound images that could be used to effectively differentiate between benign and malignant breast tumors. An algorithm has been developed to extract such features based on three steps. During the preprocessing stage filters, image enhancement techniques as well as morphological operators were utilized. The feature extraction stage allowed to extract statistical features derived based on power spectra of the 2D Stockwell transform for effective edge detection and segmentation of breast tumors. The final classification utilized ANN with appropriate training and testing stages.

In order to quantify the performance of the proposed scheme, different matrices were used including overall accuracy, AUC values and Canberra distance. Five features were first calculated from the ultrasound images and inputted into the ANN classifier and the performance of the features in differentiating benign and malignant breast tumors was evaluated by comparing it against available gold standard (ground truth). These features were mean intensity, variance, STD, entropy and contrast. The overall accuracy was found to be around 90% and the classification performance resulted in an AUC value close to 0.99 showing the great promises of the proposed algorithm. Comparison was made between individual features against their combination using ANN and it was found that the combination of the five features using ANN offered a result which is much superior compared to individual features.

6.2 Future Works

The research that has been undertaken in this thesis has highlighted a number of topics on which further research would be beneficial. For instance, there are still rooms to improve the performance of the segmentation. This could be as a result of deficient preprocessing technique. A more accurate segmentation could result in improved classification accuracy by the proposed method. Furthermore, in this study, the number of sample images taken for training and testing was limited. Incorporating more samples could improve the classification performance. These issues await further investigations.

Bibliography

[1] P. Palanikumar, S. Geofrin Shirly, and S. Balakrishnan, “An effective two way classification of breast cancer images,” *International Journal of Applied Engineering Research*, vol. 1, no. 1, pp. 78–81, 2015.

[2] Shallu and R. Mehra, “Breast cancer histology images classification: Training from scratch or transfer learning,” *ICT Express*, vol. 1, no. 1, p. 17, 2018.

[3] S. Nivins, “Breast cancer detection of ultrasound image using watershed technique A Monthly Double-Blind Peer Reviewed Refereed Open Access International e-Journal-Included in the International Serial Directories,” *ResearchGate*, vol. 3, no. 4, pp. 54–57, 2017.

[4] R. Srisha, “1st International Mediterranean Science and Engineering Congress,” Adana,Turkey: October 26-28,2016, 2017.

[5] I. El-Hasnony, H. M. El-Bakry, and A. A. Ibrahim M Saleh, “Classification of Breast Cancer Using Softcomputing Techniques,” *International Journal of Electronics and Information Engineering*, vol. 4, no. 1, pp. 45–54, 2016.

[6] X. Shi, H. D. Cheng, L. Hu, W. Ju, and J. Tian, “Detection and classification of masses in breast ultrasound images,” *Digital Signal Processing: A Review Journal*, vol. 20, no. 3, pp. 824–836, 2010.

[7] H. D. Cheng, J. Shan, W. Ju, Y. Guo, and L. Zhang, “Automated breast cancer detection and classification using ultrasound images: A survey,” *Pattern Recognition*, vol. 02, no. 1, pp. 11–12, 2010.

[8] S. Punitha, A. Amuthan, and K. S. Joseph, “Benign and Malignant Breast Cancer Segmentation Using Optimized Region Growing Technique,” in *Future Computing and Informatics Journal*, vol. 02, no. 1, 2018, pp. 11–19.

[9] W. Nawaz, S. Ahmed, A. Tahir, and H. A. Khan, “Classification Of Breast Cancer Histology Images Using ALEXNET,” vol. 3, no. 1, 2018, pp. 33–47.

[10] X. Liu, J. Shi, S. Zhou, and M. Lu, “An iterated Laplacian based semi-supervised dimensionality reduction for classification of breast cancer on ultrasound images,” in *2014 36th Annual International Conference of the IEEE Engineering in Medicine and Biology Society, EMBC 2014*, 2014, vol. 1, no. 1, pp. 71–73.

[11] R. Guo, G. Lu, B. Qin, and B. Fei, “Ultrasound Imaging Technologies for Breast Cancer Detection and Management: A Review,” *Ultrasound in Medicine and Biology*, vol. 1. pp. 8–12, 2018.

[12] H. D. Cheng, “Global Cancer Observatory,” *Digital Times*, vol. 12, no. 1, pp. 10–23, 2012.

[13] R. V. Menon, P. Raha, S. Kothari, S. Chakraborty, I. Chakrabarti, and R. Karim, “Automated detection and classification of mass from breast ultrasound images,” in *2015 5th National Conference on Computer Vision, Pattern Recognition, Image Processing and Graphics, NCVPRIPG 2015*, 2016, vol. 02, no. 02, pp. 4–7.

[14] N. D. Khalilabad, H. Hassanpour, and M. R. Abbaszadegan, “Fully automatic classification of breast cancer microarray images,” *Journal of Electrical Systems and Information Technology*, vol. 1, no. 1, pp. 11–17, 2016.

[15] R. Fadil *et al.*, “Early Detection of Breast Cancer Using Ultrasound Imaging Development of the 3rd Generation Al-Li Alloys in Aeronautic Industry : From Material by Design to optimization of the final Aircraft Shape View project West Nile Virus-Data Mining View project,” 2018.

[16] A. Ibrahim, S. Mohammed, and H. A. Ali, “Breast Cancer Detection and Classification Using Thermography: A Review,” in *Advances in Intelligent Systems and Computing*, 2018, vol. 02, no. 1, pp. 10–16.

[17] S. Z. A. A. Abdelshafy, M. M. Refaat, G. E. Saleh, and M. I. Yousef, “Value of intra-

operative ultrasound in localization of palpable or non-palpable breast tumors during breast conserving surgery," *Egyptian Journal of Radiology and Nuclear Medicine*, vol. 1, no. 1, pp. 23–29, 2018.

[18] P. Bethapudi, E. Sreenivasareddy, and T. Sitamahalakshmi, "A Computational Approach for Better Classification of Breast Cancer using GeneticAlgorithm," 2015.

[19] Y. Guo, "Computer-Aided Detection of Breast Cancer Using Ultrasound Images Neutrosophic Machine Learning View project Computer Aided Detection View project," 2014.

[20] A. M. Sayed, E. Zaghloul, and T. M. Nassef, "Automatic Classification of Breast Tumors Using Features Extracted from Magnetic Resonance Images," in *Procedia Computer Science*, 2016, vol. 1, no. 1, pp. 19–24.

[21] B. Kirthika, P. Malathi, C. L. Y. Sivakumari, and P. Sudharsan, "A comparative analysis of de-noising techniques in ultrasound B mode images," *International Journal of Advanced Research in Computer and Communication Engineering*, vol. 3, no. 1, pp. 5136–5140, 2014.

[22] D. Saslow, C. Boetes, and W. Burke, "American Cancer Society Breast Cancer Advisory Group. American Cancer Society guidelines for breast screening with MRI as an adjunct to mammography," *CA Cancer J Clin*, vol. 57, no. 2, p. 75, 2007.

[23] S. Lidar and T. Cuhaf, "Manual of Diagnostic Ultrasound," *IEEE Engineering in Medicine and Biology Magazine*, vol. 1, no. 1, pp. 5–8, 2016.

[24] K. A. Haseena and K. K. Sherikhh, "A View on Ultrasonogram Denoising Techniques," *Clinical Ultrasound*, vol. 1, no. 1, pp. 18–23, 2012.

[25] Essential Health Technologies, "BASIC PHYSICS ULTlVlSONOGRAPHIC," .

[26] T. Gudra, J. Furmankiewicz, and K. Herman, "Bats Sonar Calls and Its Application in Sonar Systems," *science direct*, vol. 2, no. 1, pp. 14–18, 2004.

[27] B. Idea, “Basic ultrasonic and sound waves,” *History*, vol. 1, no. 3, pp. 1–24, 1965.

[28] J. E. Aldrich, “Basic physics of ultrasound imaging,” *Medical Physics*, vol. 35, no. 5, pp. 131–137, 2007.

[29] T. Physics, “The Physics of Sound,” *Medical Physics*, vol. 1, no. 2, pp. 30–37, 2015.

[30] P. Laugier and G. Ha, “Introduction to the Physics of Ultrasound,” *ResearchGate*, vol. 2, no. May 2014, pp. 56–73, 2010.

[31] W. N. Mcdicken and T. Anderson, *Basic physics of medical ultrasound*, Thrid Edit., vol. 2. Elsevier Ltd, 2013.

[32] R. Horan and M. Lavelle, “Introduction to Waves Table of Contents,” *Molecular Pathology of Breast Cancer*, vol. 1, no. 2, pp. 1–34, 2008.

[33] U. Waves, *Ultrasound waves*, vol. 2. 2002.

[34] G. Saddik, “Ultrasound Imaging System,” *Medical Physics*, vol. 3, no. 2, pp. 45–47, 2015.

[35] A. Definitions, “Ultrasonic Transducers Technical Notes,” *science direct*, vol. 3, no. 1, pp. 39–49, 2016.

[36] M. Genovese and R. Rt, “Ultrasound Transducers,” *IEEE Engineering in Medicine and Biology Magazine*, vol. 1, no. 2, pp. 23–27, 2016.

[37] W. Nawaz, S. Ahmed, A. Tahir, and H. A. Khan, “Classification Of Breast Cancer Histology Images Using ALEXNET,” vol. 02, no. 1, 2018, pp. 6–9.

[38] X. Ho, “Breast Anatomy and Physiology Unit 1 Key to Quality Mammograms,” vol. 1, no. 1, 2016, pp. 31–36.

[39] S. Chucherd and S. S. Makhanov, “Multiresolution phase portrait analysis for segmentation of ultrasound images for detection of breast cancer,” *IMECS 2011 - International MultiConference of Engineers and Computer Scientists 2011*, vol. 1, no. May, pp. 33–39,

2011.

[40] Alaska Regional Hospital, “Breast Density,” vol. 1. p. 39, 2015.

[41] A. C. R. Bi-rads, “American College of Radiology,” 2012.

[42] L. Medina-Valdés, M. Pérez-Liva, J. Camacho, J. M. Udías, J. L. Herraiz, and N. González-Salido, “Multi-modal Ultrasound Imaging for Breast Cancer Detection,” in *Physics Procedia*, 2015, vol. 2, no. 1, pp. 44–49.

[43] N. Ozmen, R. Dapp, M. Zapf, H. Gemmeke, N. V. Ruiter, and K. W. A. Van Dongen, “Comparing different ultrasound imaging methods for breast cancer detection,” *IEEE Transactions on Ultrasonics, Ferroelectrics, and Frequency Control*, vol. 1, no. 1, pp. 1–17, 2015.

[44] J. Zubovits, “Global Cancer Observatory,” *Web page*, vol. 1, no. 1, pp. 1–14, 2011.

[45] P. Hamsagayathri and P. Sampath, “Decision Tree Classifiers for Classification of Breast Cancer,” *International Journal of Current Pharmaceutical Research*, vol. 1, no. 1, pp. 33–35, 2017.

[46] ACS, “Breast Cancer Early Detection and Diagnosis American Cancer Society Recommendations for the Early Detection of Breast Cancer,” *American Cancer Society*, vol. 1, no. 1, pp. 17–19, 2016.

[47] L. Medina-Valdés, M. Pérez-Liva, J. Camacho, J. M. Udías, J. L. Herraiz, and N. González-Salido, “Multi-modal Ultrasound Imaging for Breast Cancer Detection,” in *Physics Procedia*, 2015, vol. 1, no. 1, pp. 44–56.

[48] F. M. Osman and M. H. Yap, “The effect of filtering algorithms for breast ultrasound lesions segmentation,” *Informatics in Medicine Unlocked*, vol. 1. pp. 15–23, 2018.

[49] “American Cancer Society Cancer Action Network | Home.” [Online]. Available: https://www.fightcancer.org/. [Accessed: 29-Dec-2018].

[50] L. Zhang, "Breast Ultrasound Image," *Clinical Ultrasound*, vol. 1, no. 1, pp. 7–14, Dec. 2017.

[51] M. R. Imaging and D. Mri, "MRI of the Breast," 2014.

[52] B. K. Singh, K. Verma, and A. S. Thoke, "Adaptive gradient descent backpropagation for classification of breast tumors in ultrasound imaging," in *Procedia Computer Science*, 2015, vol. 1, no. 1, pp. 33–38.

[53] M. Xian, Y. Zhang, H. D. Cheng, F. Xu, B. Zhang, and J. Ding, "Automatic breast ultrasound image segmentation: A survey," *Pattern Recognition*, vol. 1, no. 1, pp. 9–13, 2018.

[54] T. Iesmantas and R. Alzbutas, "Convolutional Capsule Network for Classification of Breast Cancer Histology Images," in *Lecture Notes in Computer Science (including subseries Lecture Notes in Artificial Intelligence and Lecture Notes in Bioinformatics)*, 2018, vol. 10882 LNCS, no. 1, pp. 853–860.

[55] Y. Su, Y. Wang, J. Jiao, and Y. Guo, "Automatic detection and classification of breast tumors in ultrasonic images using texture and morphological features.," *The open medical informatics journal*, vol. 5, no. Suppl 1, pp. 26–37, 2011.

[56] N. Walia, S. Makkar, and M. Kumar, "Classification of Breast Cancer Tissues using Decision Tree Algorithms Predicting Students Academic Performance using Data Mining Techniques: A Case Study View project IMAGE PROCESSING View project Classification of Breast Cancer Tissues using Decision Tr," *International Journal for Research in Engineering Application & Management (IJREAM)*, vol. 04, no. 1, p. 5, 2018.

[57] A. Osmanović, S. Halilović, L. A. Ilah, A. Fojnica, and Z. Gromilić, "Machine learning techniques for classification of breast cancer," in *IFMBE Proceedings*, 2019, vol. 1, no. 1, pp. 17–21.

[58] D. Assefa, H. Keller, C. Ménard, N. Laperriere, R. J. Ferrari, and I. Yeung, "Robust texture

features for response monitoring of glioblastoma multiforme on T 1-weighted and T 2-FLAIR MR images : A preliminary investigation in terms of identification and segmentation," *Medical Physics*, vol. 37, no. 2, pp. 1722–1736, 2010.

[59] A. and M. S. S. Rodtook, "Medical Images Home," *science direct*, 2015. [Online]. Available: http://www.onlinemedicalimages.com/index.php/en/. [Accessed: 18-Dec-2018].

[60] O. Magud, E. V. A. Tuba, and N. Bacanin, "Medical Ultrasound Image Speckle Noise Reduction by Adaptive Median Filter," *science direct*, vol. 14, no. 1, pp. 38–46, 2017.

[61] P. S. Hiremath, P. T., and S. Badiger, "Speckle Noise Reduction in Medical Ultrasound Images," *Advancements and Breakthroughs in Ultrasound Imaging*, vol. 2, no. 1, pp. 15–28, 2013.

[62] Y. Wang, "Efficient Stockwell Transform with Applications to Image Processing by," *IEEE Transactions on Ultrasonics, Ferroelectrics, and Frequency Control*, vol. 3, no. 1, pp. 12–23, 2011.

[63] R. G. Stockwell, L. Mansinha, and R. P. Lowe, "Localization of the complex spectrum: the S transform," *IEEE Transactions on Signal Processing*, vol. 44, no. 4, pp. 998–1001, Apr. 1996.

[64] L. Yun, X. Xiaochun, L. Bin, and P. Jinfeng, "Time-frequency Analysis Based on the S-transform," *International Journal of Signal Processing, Image Processing and Pattern Recognition*, vol. 6, no. 5, pp. 245–254, 2013.

[65] A. Mansour, "Kurtosis : Definition and Properties," *science direct*, vol. 1, no. November 2012, pp. 11–17, 2000.

[66] R. Srisha and a M. Khan, "Morphological Operations for Image Processing : Understanding and its Applications Morphological Operations for Image Processing : Understanding and its Applications," *ResearchGate*, vol. 1, no. February 2015, pp. 17–19, 2013.

[67] M. L. Comer, E. J. Delp, and W. Lafayette, "Morphological Operations For Color Image

Processing,” *Journal of electronic imaging*, vol. 8, no. 3, pp. 279–289, 1999.

[68] G. Tennenholtz, T. Zahavy, and S. Mannor, “T RAIN ON V ALIDATION :,” no. 2009, pp. 1–17, 2017.

[69] D. J. Fleet and M. Brubaker, “8 Classification,” *Journal of electronic imaging*, vol. 2, no. 1, pp. 42–52, 2015.

[70] Y. Zee Ma, “Appendix_Tutorial on PCA,” *Technical Report*, vol. 2, no. February, pp. 34–53, 2014.

[71] Q. Wang, Q. Gao, X. Gao, and F. Nie, “Angle principal component analysis,” *IJCAI International Joint Conference on Artificial Intelligence*, vol. 1, no. January, pp. 2936–2942, 2017.

[72] J. Muschelli, “ROC and AUC with a Binary Predictor : a Potentially Misleading Metric arXiv : 1903 . 04881v1 [stat . CO] 12 Mar 2019,” *science direct*, vol. 1, no. 2, pp. 1–20, 2019.

[73] M. Informatics, M. Sciences, R. Kumar, and M. Informatics, “Receiver Operating Characteristic (ROC) Curve for Medical Researchers,” *ResearchGate*, vol. 2, no. 3, pp. 34–38, 2011.

[74] D. Kaur, “A Comparative Study of Various Distance Measures for Software fault prediction,” *Journal of Electrical Systems and Information Technology*, vol. 17, no. 3, pp. 117–120, 2014.

[75] R. Guo, G. Lu, B. Qin, and B. Fei, “Ultrasound Imaging Technologies for Breast Cancer Detection and Management: A Review,” *Ultrasound in Medicine and Biology*, vol. 02. pp. 2–12, 2018.

Appendix A

```
%% Reset matlab
close all; clear; clc;
%% Load original image
USI = imread('MSM_Case_10.jpg');
c = 2; % Constant for dynamic figure numbering
figure(c), imshow(imresize(USI,[256,256])), impixelinfo, title('Original
ultrasound image')
USI_P = USI;
%% Convert to gray and Normalize
[~, ~, width] = size(USI_P);
if(width > 1)
    USI_P = mat2gray(rgb2gray(USI_P));
else
    USI_P = USI_P;
end
USI_P = im2double(USI_P);
c = c + 1; figure(c), imshow(imresize(USI_P,[256,256])), impixelinfo,
title('Normalized gray image')
orig_gray_norm = USI_P;

%%  Adjust image contrast
low_in = min(min(USI_P));       % lower intensity value
mean_in = mean(mean(USI_P));    % Mean intensity value
USI_P = medfilt2(USI_P,[5,5]);  % Median filter
USI_P = wiener2(USI_P,[5,5]);   % wiener filter
USI_P = imadjust(USI_P,[low_in mean_in],[]);
c = c + 1; figure(c), imshow(imresize(USI_P,[256,256])),impixelinfo,
title('Contrast adjusted image')
%% Apply filters
USI_P = medfilt2(USI_P,[3,3]);                        % Median filter
USI_P = wiener2(USI_P,[5,5]); gr_Wi_flt = USI_P;  % wiener filter
c = c + 1;figure(c), imshow(imresize(USI_P,[256,256]), []),
title('median+wiener filter')
med_wien_filter = USI_P;
c = c + 1;figure(c), imagesc(imresize(USI_P,[256,256])), colormap('hsv'),
title('median+wiener filter HSV')
%% Resize image for memory managment
USI_P = imresize(USI_P,[100 100]); clear I2;  % Resize original image
USI_P = imresize(USI_P,[100 100]);  % Resize filtered image
c = c + 1; figure(c), imshow(imresize(USI_P,[256,256])), impixelinfo,
title('Resized adjusted gray image')
%%  Apply Rot-inv algorithm
ss = size(USI_P);
N = ss(1); M = ss(2); %N = 64;  %M = 64;
p = 0:N-1; q = 0:M-1;
clear mek
tic
 loch = PH_rot_inv(USI_P);
toc

bbb(:,:,1,2:M/2+1) = sqrt(loch(:,:,1,2:(M/2+1)).^2+loch(:,:,1,M:-
1:(M/2+1)).^2);
```

```
bbb(:,:,2:N/2+1,1) = sqrt(loch(:,:,2:(N/2+1),1).^2+loch(:,:,N:-
1:(N/2+1),1).^2);
bbb(:,:,2:N/2+1,2:M/2+1) = sqrt(loch(:,:,2:(N/2+1),2:(M/2+1)).^2+loch(:,:,N:-
1:(N/2+1),M:-1:(M/2+1)).^2);
clear loch
ccc = kurtosis(kurtosis(bbb.^2,0,4),0,3); clear bbb
ST = USI_P/max(USI_P(:))-double(ccc)/max(ccc(:)); PH_ROt_Inv = ST; clear bbb
c = c + 1; figure(c), imshow(imresize(ST,[256,256])), title('S-Transform')
ph_rot_algthm = ST;
%% Apply 2nd time filters
ST = medfilt2(ST,[3,3]);  % Median filter
ST = wiener2(ST,[10,10]); % wiener filter
ST = im2double(ST);
c = c + 1;figure(c), imshow(imresize(ST,[256,256]), []), title('2nd
median+wiener filter')
med_wien_filter2 = ST;
c = c + 1;figure(c), imagesc(imresize(ST,[256,256])), colormap('hsv'),
title('2nd  median+wiener filter HSV')
ph_rot_algthm2 = ST;
%% 2nd stage image contrast using mean
low_in = min(min(ST));
high_in = max(max(ST));
mean_in = mean(mean(ST));
if(low_in < 0)
    low_in = 0;
end
ST = imadjust(ST,[low_in mean_in],[]);
c = c + 1; figure(c), imshow(imresize(ST,[256,256])), title('S-Transform
contrast adjusted')
%% Convert to black and white
BW = im2bw(ST);
c = c + 1;figure(c), imshow(imresize(BW,[256,256])), title('Convert image to
BW')
%% Morphological operation
BWC = imcomplement(BW);
c = c + 1;figure(c), imshow(imresize(BWC,[256,256])),
title('BW\_imcomplement')
BWCF = imfill(BWC,'holes');
c = c + 1;figure(c), imshow(imresize(BWCF,[256,256])), title('Fill image
hole')
BWCFAO = bwareaopen(BWCF, 50);
c = c + 1;figure(c), imshow(imresize(BWCFAO,[256,256])), title('Remove
unkwanted small regions')

%% Edge detection
sim = edge(BWCFAO,'canny');
c = c + 1;figure(c), imshow(imresize(sim,[256,256])), title('Edge detected')
BWCFAOF = imfill(sim,'holes');
c = c + 1;figure(c), imshow(imresize(BWCFAOF,[256,256])), title('Fill image
hole')
BWCFAOFAO = bwareaopen(BWCFAOF, 50);
c = c + 1; figure(c), imshow(imresize(BWCFAOFAO,[256,256])), title('Remove
unkwanted small regions')
[roi_r, roi_c] = find(BWCFAOFAO == 1);
roi_val = zeros(1,length(roi_r));
w = 1;
```

```
for v = 1:length(roi_r)
    roi_val(1,v) = roi_val(1,v) + USI(roi_r(v),roi_c(w),1);
    w = w + 1;
end
%% Calculate features
roi_avg = mean(roi_val);          % ROI mean
roi_var = var(roi_val);           % ROI variance
roi_entropy = entropy(roi_val); % ROI entropy
roi_contrast = sqrt(1/numel(roi_val)*sum(power((roi_val(:)-
mean(roi_val(:))),2))); % ROI contrast

[bkd_r, bkd_c] = find(BWCFAOFAO == 0);
bkd_val = zeros(1,length(bkd_r));
w = 1;
for v = 1:length(bkd_r)
    bkd_val(1,v) = bkd_val(1,v) + USI(bkd_r(v),bkd_c(w),1);
    w = w + 1;
end
bkd_avg = mean(bkd_val);
bkd_var = var(bkd_val);
int_ratio_roi_bkd = roi_avg/bkd_avg;  % Mean ratio
var_ratio_roi_bkd = roi_var/bkd_var;  % Variance ratio
if int_ratio_roi_bkd <= 0.4
    disp('Based on Intensity Ratio');
    disp([' --Malignant---Ratio=',num2str(int_ratio_roi_bkd)]);
else
    disp('Based on Intensity Ratio');
    disp([' --Benign---Ratio=',num2str(int_ratio_roi_bkd)]);
end
if var_ratio_roi_bkd <= 0.4
    disp('Based on Variance Ratio');
    disp(['---Malignant---Ratio=',num2str(var_ratio_roi_bkd)]);
else
    disp('Based on Variance Ratio');
    disp(['---Benign---Ratio=',num2str(var_ratio_roi_bkd)]);
end
%% Contour image
BWCFAOFAOPM = bwperim(BWCFAOFAO,8);
BWCFAOFAOPM = imresize(BWCFAOFAOPM,[256,256]);
c = c + 1;figure(c), imshow(BWCFAOFAOPM), title('Show perimeter')
[rf, cf] = find(BWCFAOFAOPM ==1);
w = 1;
I2_cr = USI;
USI = imresize(USI,[256,256]);
for v = 1:length(rf)
    if(width > 1)
        USI(rf(v),cf(w),:) = [0 256 0];
    else
        USI(rf(v),cf(w)) = 255;
    end
    w = w + 1;

end
c = c + 1; figure(c), imshow(imresize(USI,[256,256])); impixelinfo,
title('Segmented image')
%% Show results in group
```

```
c = c + 1; ax0 = figure(c);
set(ax0, 'Color',[1,1,1]);
subplot(2,2,1); imshow(imresize(I2_cr,[256,256])), title('Original cropped
image'), axis off;
subplot(2,2,2); imshow(imresize(PH_ROt_Inv,[256,256])), title('After
filters'), axis off;
ax3 = subplot(2,2,3); imshow(PH_ROt_Inv), colormap(ax3,hsv),  title('S-
Transform'), axis off;
subplot(2,2,4); imshow(imresize(USI,[256,256])),title('Final contour image'),
axis off;
```